

Microwave radiometry experiment for snow in Altay China: time series of *in situ* data for electromagnetic and physical features of snow pack

Liyun Dai¹, Tao Che^{1,2*}, Yang Zhang¹, Zhiguo Ren^{1,3}, Junlei Tan¹, Meerzhan Akynbekkyzy¹, Lin Xiao¹, Shengnan Zhou¹, Yuna Yan³, Yan Liu⁴, Hongyi Li¹, Lifu Wang⁵

¹Key Laboratory of Remote Sensing of Gansu Province, Heihe Remote Sensing Experimental Research Station, Northwest Institute of Eco-Environment and Resources, Chinese Academy of Sciences, Lanzhou, 730000, China.

²Center for Excellence in Tibetan Plateau Earth Sciences, Chinese Academy of Sciences, Beijing, 100101, China.

³University of Chinese Academy of Sciences, Beijing, 1000101, China.

⁴ Institute of Desert Meteorology, China Meteorological Administration, Urumqi, 830002, China

⁵Altay National Reference Meteorological station, China Meteorological Administration, Altay, 836500, China.

Correspondence to: Tao Che (chetao@lzb.ac.cn)

~~Abstract. Snow depth is a key parameter in climatic and hydrological systems. Passive microwave remote sensing, snow process model and data assimilation are the main methods to estimate snow depth in large scale. The estimation accuracies strongly depend on input of snow parameters or characteristics. snow depth. Because the evolving processes of snow parameters vary spatiotemporally, and are difficult to accurately simulate or observe, large uncertainties and inconsistency exist among existing snow depth products. Therefore, a comprehensive experiment is needed to understand the evolution processes of snow characteristics and their influence on microwave radiation of snowpack, to evaluate and improve the snow depth and SWE retrieval and simulation methods. In this paper, we present a comprehensive experiment, namely, An Integrated Microwave Radiometry Campaign for snow (IMCS), was conducted at the Altay National Reference Meteorological station (ANRMS) in Xinjiang, China, during snow season of 2015/2016. The campaign hosted a dual polarized microwave radiometer operating at L, K and Ka bands to provide minutely passive microwave observations of snow cover at a fixed site, along with daily manual snow pit observation of snow physical parameters measurements, automatic observation of ten-minute 4-component radiation and layered snow temperatures, and meteorological observation of hourly weather data and soil data ten-minute automatic 4-component radiation and layered snow temperatures, covering a full snow season of 2015/2016. The measurements of meteorological and underlying soil parameters were requested from the ANRMS. This study provides a summary of the obtained data, detailing measurement protocols for microwave radiometry, in situ snow pit and station observation data. A brief analysis of the microwave signatures against snow parameters is presented. These data were consolidated into five NetCDF files and A consolidated dataset of observations, comprising the ground passive microwave brightness temperatures, in situ snow characteristics, 4-component radiation and weather parameters, was achieved at the National Tibetan Plateau Data Center,~~

~~China. To the best of our knowledge, our~~The dataset is unique in providing continuous daily snow pits data and coincident microwave brightness temperatures, radiation and meteorological data, at a fixed site over a full season~~—, which can be straightforwardly used for The dataset is expected to serve the~~ evaluation and development of microwave radiative transfer models and snow process models~~—, along for land surface process and hydrology models.~~ The consolidated data are available at <http://data.tpdc.ac.cn/zh-hans/data/df1b5edb-daf7-421f-b326-cdb278547eb5/> (doi: 10.11888/Snow.tpdc.270886) (Dai, 2020).

Key words: Snow, Microwave radiometry, Snow pit, Experiment

1 Introduction

~~Seasonal snow cover plays a critical role in climate and hydrological systems (Cohen, 1994; Ding et al., 2020; Barnett et al., 2005; Immerzeel et al., 2010) by its high albedo, thermal insulation, fresh water reserves and its phase change processes. Snow cover can be accurately identified by optical remote sensing. However, the snow surface albedo is controlled by snow characteristics (Aoki et al., 2003 and 2000), and variations in snow characteristics cause uncertainties in albedo estimation. Snow depth and snow water equivalent (SWE) are currently estimated using passive microwave at global and regional scales (Pullianen et al., 2020; Tedeseo and Narvekar, 2010; Jiang et al., 2014; Che et al., 2008). Although several global and regional snow depth and SWE products have been released, large uncertainties exist in these products because of the spatio-temporal variations in snow characteristics (Xiao et al., 2020; Mortimer et al., 2020; Che et al., 2016; Dai et al., 2012; Dai and Che, 2022). Therefore, the observation of electromagnetic and physical parameters of snowpack are necessary to improve understanding of the electromagnetic radiation process of snowpack to enhance the estimation accuracy of snow surface albedo and snow depth.~~

~~Field experiments/campaigns, as the main and most important approach for snow studies. To evaluate and improve snow depth and SWE retrieval methods from passive microwave remote sensing observations and to combine remote sensing technologies with modeling and data assimilation methods to produce the most accurate products, a few large or systematic experiments or campaigns have been conducted to obtain the —on~~electromagnetic and physical characteristics measurement of snow cover. The ~~mainse~~ experiments/campaigns are summarized in table 1. The Cold Land Processes Field Experiment (CLPX) (<https://nsidc.org/data/clpx/index.html>), one of the most well-known experiments, was carried out from winter of 2002 to spring of 2003 in Colorado, USA (Cline et al., 2003). During the campaign, snow pits were collected ~~in February and March of 2002 and 2003~~ to coincide with airborne and ground remote sensing observations. ~~In 2017,~~ NASA SnowEx campaign (<https://nsidc.org/data/snowex>) was conducted ~~in 2017~~ in ~~Colarado~~Colorado to test and develop algorithms for measurement of SWE in forested and non-forested areas by providing multi-sensor observations of seasonally snow-covered landscapes (Brucker et al., 2017). The campaign is still ongoing and will be conducted in other areas with different snow conditions. In northern Canada, mobile sled-mounted microwave radiometers were deployed in forest, open and lake environments from November 2009 to April 2010 and snow characteristics within the footprints of radiometers were measured to improve ~~the~~ understanding ~~of~~ the influence of snow characteristics on brightness temperatures (Derksen et al., 2012; Roy et al., 2013). ~~These aforementioned~~ microwave experiments ~~were of mobile observation.~~ ~~The observations were conducted at different~~ ~~In these experiments, there were multiple observation~~ sites

for different land cover, ~~resulting in good representativity for evaluating snow microwave emission model (Tedesco and Kim, 2006; Royer et al., 2017), however, with relative short temporal range, while dense temporal resolution is important to reveal the evolution of snow characteristics~~but relative short temporal range. The snow pit observations were used ~~to aimed at evaluate evaluating snow microwave emission model in different land cover (Tedesco and Kim, 2006; Royer et al., 2017), but they did could not exhibit the evolution of snow parameters.~~

In the Arctic region, the Nordic Snow Radar Experiment (NoSREx) campaign was conducted at a fixed field ~~of the Arctic boreal forest area~~ in Sodankylä, Finland, during 2009 ~ 2013 (Lemmetyinen et al., 2016). This experiment provided a ~~continuous time series of active and passive microwave observations of snow cover at a representative location of the Arctic boreal forest area~~ spanning an entire winter season, ~~with synchronous observations of and matched snow pit observations were made~~ weekly. In Asia, ~~an experiment of radiation budget over snow cover (JERBES) was conducted in Japan. In the experiment,~~ snow pit work at 3 or 4 day intervals was conducted simultaneously with radiation budget observations during winter of 1999/2000 and 2000/2001 to analyze the effects of snow physical parameters on albedo (Aoki et al., 2003). The NoSREx and ~~JERBES Japan radiation~~ experiments, ~~were for fixed field observation, which provided longer improved time series of data than CLPX and SnowEx. These experiments were conducted in deep snow areas, and the w~~Weekly observation could reflect general evolution process of snow characteristics but might miss some key details that occur at sub-weekly scales. In the Tibetan plateau with shallow snow cover, multiple years of microwave radiometry observation at L band were conducted to study passive microwave remote sensing of frozen soil (Zheng et al., 2019, ~~and 2021a and; Zhang et al., 2021b~~). However, in the long-term series of experiment, no snow pit was measured and the microwave radiometry observation was performed at L band which is insensitive to snowpack.

Table 1. Summary of existing experiments for microwave and optical radiation and physical features of snowpack

Campaign	Location	Temporal range	Observation content
CLPX	Different sites in Colorado,	February and March of 2002 and 2003	Inconsecutive multiple sensor observation, including microwave radiometry over snow, and and matched synchronous snow pit measurements were conducted at different sites with short temporal range. ---
SnowEx-year 1	Grand Mesa, and Senator Beck Basin, Colorado	February of 2017	Inconsecutive multiple sensor observation, including microwave radiometry over snow, and matched synchronous snow pit measurements were conducted at different sites with short temporal range. ---
CMRES ¹	Mobile observation at Forest, open and lake in the northern Canadian region	November of 2009-April of 2010	Mobile microwave radiometry and snow pit observation within footprint of radiometer. Short temporal range and inconsecutive observation

NoSREx	Fixed site in Sodankylä, Finland	Snow season during 2009-2013	Consecutive microwave radiometry and SAR observation over snow, and weekly snow pit measurement
JERBS ²	Fixed site in Japan	Snow season during 1999-2000	Consecutive optical radiation observation over snow and consecutive snow pit measurement at 3 or 4-day interval-
IMCS_ (Presented in this work)	Fixed site in China	November of 2015-March of 2016	Consecutive microwave radiometry and optical radiation observation, and consecutive daily snow pit measurements-

Note: ¹CMRES: Microwave radiometry experiment on snow cover conducted in northern Canada

²JERBS: ~~Experiment of radiation budget over snow cover in Japan~~

To understand the evolution of snow characteristics and their influence on passive microwave brightness temperatures and radiation budget, an integrated [field](#) experiment on snowpack was conducted during a full snow season, in Altay, China. The experiment was designed to cover periods from snow-free conditions to eventual snow melt-off during 2015/2016. The microwave radiometry measurements at L, K and Ka bands for multiple angles were complemented by a dual-polarized microwave radiometer with 4-component radiation and daily in situ observations of snow, soil and atmospheric properties, using both manual and automated methods. To the best of our knowledge, our dataset is unique in providing continuous daily snow pit observations over a full snow season at a fixed site, along with synchronous microwave brightness temperatures, radiation and meteorological data. The dataset ~~of electromagnetic and physical parameters were~~ is ~~further~~ consolidated and organized, ~~which can be to be~~ easily read and utilized ~~used~~ for other researchers with interests.

~~The dataset is unique in providing continuous daily snow pits data over a snow season at a fixed site and matched microwave brightness temperatures, radiation and meteorological data.~~ In the next section, the experiment location, parameters, and parameter measurement protocols are described; ~~section-Section 3~~ introduces the consolidated data which was released at the National Tibetan Plateau Data Center, China; ~~section-Section 4~~ presents content of brightness temperature, 4-component radiation, snow pit data, soil temperature and moisture, and meteorological data; ~~section-Section 5~~ discusses the possible applications and uncertainties; ~~and finally~~ the conclusions are summarized in section 6.

2 Description of experiment setup

2.1 Measurement location

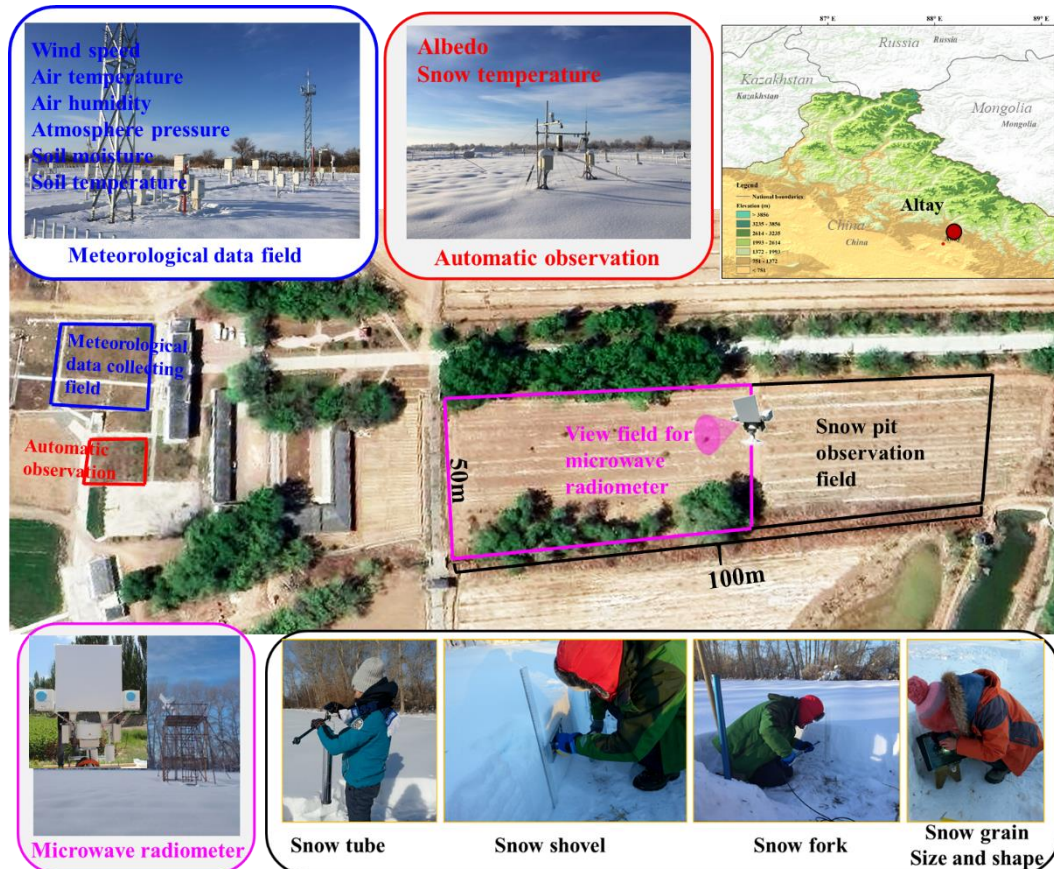
The Integrated Microwave Radiometry Campaign for snow (IMCS) was performed during the 2015/2016 snow season (from November 27, 2015 to March 25, 2016) at the Altay National Reference Meteorological station (ANRMS) (N47°44'26.58", E 88°4'21.55"), which is approximately 6 km from the foot of Altay mountain in the northwest China (Figure 1). Altay mountain with elevation up to 3000 m, running northwest and southeast, is at the junction of China, Russia, Mongolia and Kazakhstan, ~~and~~ provides [sing](#) snow water resources for these four countries. The average annual maximum snow depth measured in this station is approximately 40 cm, with a maximum over 70 cm. In the southwest of Altay

138 mountain, crop land and desert with flat terrain are the dominant land covers. Snow cover is critical fresh
139 water for the irrigation in this area. In this experiment, measurements included microwave radiometry,
140 4-component radiation, snow pit and soil parameters. The test sites of this experiment ~~was-were~~ four
141 neighboring bare rectangle fields in the ANRMS with areas of 2500_m² (black rectangle field in Figure
142 1), 2500_m² (pink rectangle field in Figure 1), 200_m² (red rectangle field in Figure 1) and 400 m² (blue
143 rectangle field in Figure 1), respectively.

144 In the pink field, the ground-based microwave radiometer was set up in the middle of the field,
145 facing south to collect brightness temperatures ~~of over~~ snow cover. The black field behind the microwave
146 radiometers (north of the radiometers) was for manual snow pit data collection. The microwave
147 radiometer observations and snow pit data collections were conducted by Northwest Institute of Eco-
148 Environment and Resources, Chinese Academy of Science (NIEER) from November 27, 2015 to March
149 25, 2016 (~~snow free a~~After March 25, 2016, ~~snow melted out~~).

150 The blue field was for meteorological measurements including wind speed, wind direction, air
151 temperature, air wetness, air pressure, precipitation, soil temperature, soil moisture among others. These
152 parameters were automatically obtained from instruments, and the instruments setup and data collection
153 were operated by ANRMS. ~~This station also has daily manual observation of snow depth and SWE.~~ In
154 this experiment, we requested the wind, air pressure, air wetness, air pressure, soil temperature and
155 moisture data during this experiment from ANRMS. The red field was designed for automatic
156 measurement of layered snow temperatures, snow density, SWE, snow depth, and albedo, ~~with These~~
157 ~~automatic measurement~~ instruments ~~were installed and maintained~~operated by NIEER, ~~and started~~
158 ~~working from since~~ 2013. However, during the experiment, the instruments for snow density and SWE
159 ~~did not work~~were not functional, and we only collected layered snow temperatures and 4-component
160 radiation.

161 ~~Because~~ ~~Because~~ ~~the~~ the four observation fields ~~are~~ located within the domain of the station, ~~are and~~
162 ~~the distance between them are~~ with distance less than 100_m, ~~it is reasonable to assume that~~ the snow
163 characteristics and soil and weather conditions are ~~thought to be the same~~consistent among these four
164 fields. Overall, ~~the experiment performed a systematic observation covering electromagnetic and~~
165 ~~physical features of snow pack, providing data for studies on snow remote sensing and models.~~



166

167 **Figure 1.** Location of the Altay National Reference Meteorological station (ANRMS) in Asia, along with ~~and~~
 168 ~~the distribution of the three-four test sites/experiment fields~~ in the ANRMS. The black rectangle field
 169 (approximately 40 m × 50 m) ~~represents the field used for snow characteristics (approximately 40 m × 50 m)~~
 170 ~~including was for~~ snow layering, layer thickness, snow density, snow grain size and shape of each layer. The
 171 pink rectangle (approximately 60 m × 50 m) ~~was for, and~~ microwave radiometers (approximately 60 m × 50
 172 m) ~~observations~~. The blue rectangle field is was the field ~~is was the field~~ for meteorological and soil data collection operated
 173 by the ANRMS. The red rectangle field was is ~~field was is~~ for the automatically observation of the snow temperature, and
 174 4-component radiation, designed by Northwest Institute of Eco-Environment and Resources, Chinese
 175 Academy of Science (NIEER).

176 **2.2 Measurement methods**

177 The microwave signatures from snowpack vary with snow characteristics, soil and weather
 178 conditions. In this experiment, the measurements include microwave radiometry observation to collect
 179 brightness temperature, manual snow pit observation to collect snow physical parameters, automatic
 180 observation to collect 4-component radiation and snow temperatures, and meteorological observation
 181 ~~which contains~~ containing weather data and soil data.

182 **2.2.1. Microwave radiometry**

183 The brightness temperatures at 1.4 GHz, 18.6 GHz, and 36.5 GHz for both polarization (Tb1h, Tb1v,
 184 Tb18h, Tb18v, Tb36h, Tb36v) were automatically collected using a six-channel dual polarized
 185 microwave radiometer RPG-6CH-DP (Radiometer Physics GmbH, Germany,
 186 <https://www.radiometerphysics.de/products/microwave-remote-sensing-instruments/radiometers/>). The

187 technical specifications of the RPG-6CH-DP are described in Table 2. The RPG-6CH-DP contains a
 188 built-in temperature sensor ~~which caused for~~ measuring air temperature. The automated data collection
 189 frequency was set to 1 minute.

190

191 **Table 2. Technical Specifications of the RPG-6CH -DP Microwave Radiometer.**

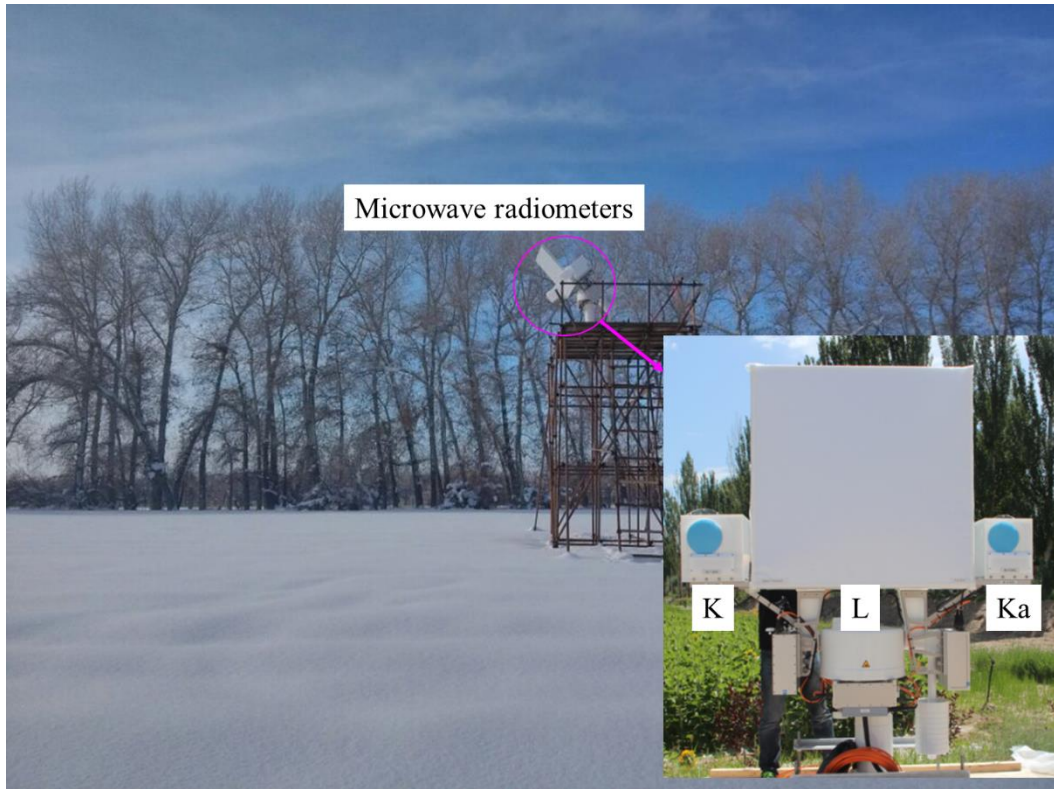
Parameter	Value
Manufacturer	Radiometer Physics GmbH
System noise temperatures	<900 K
Bandwidth	400MHz (20MHz for 1.4 GHz)
System stability	0.5 K
Dynamic range	0~400 K
Frequencies (GHz)	1.4, 18.7, 36.5
Polarizations	V, H
Internal calibration	Internal Dicke switch and software control for automatic sky tilt calibration
Receiver and antenna thermal stabilization	< 0.015 K
Antenna sidelobe level	< -30 dBc
Optical resolution (HPBW)	6.1° (11° for 1.4 GHz)
Incidence angle	0~90°
Azimuth angle	360°

192

193 Before the snow season, a platform with height of 5 m, length of 4 m and width of 2 m was
 194 constructed in the experiment field (Figure 2). A 4-m orbit was fixed on the platform. The RPG-6CH-DP
 195 was set up on the orbit and could be moved along the orbit. The microwave radiometers at K and Ka
 196 bands began working from November 27, 2015, ~~but while~~ the L band radiometer ~~did not began~~ working
 197 ~~since until~~ January 30, 2016. These radiometers were sky tipping calibrated, ~~and the calibration with~~
 198 accuracy ~~is of~~ 1 K. In clear sky conditions, the sky brightness temperatures were approximately 29.7 ± 0.3
 199 K at 18.7 GHz ~~for both polarizations~~ and 29.3 ± 0.9 K at 36.5 GHz for both polarizations. ~~But While~~ the
 200 sky brightness temperatures at L band showed large fluctuation. They ranged from -1 to 8 K for horizontal
 201 polarization, and 1 to 16 K for vertical polarization.

202

203 Generally, the radiometers were fixed in the middle of the orbit to observe snow cover with incidence
 204 angle of 50°. Multi-angle observations were conducted after every big snowfall, ~~or and~~ every 5 days in
 205 the stable period. In the melt period, observation frequency increased. There are total seventeen multi-
 206 angle observation (~~on~~ December 3, 19, and 30; January 3, 8, 13, 18, 3, and 28; February 3; March 3, 10,
 207 15, 22, 26, 28, and 31,) when the radiometer was set to scan the ground at different incidence angles at
 208 ~~two ends and the middle~~ the left, middle and right ~~and the middle place of the orbit,~~
 209 ~~respectively~~. Although the view fields of the antennas for 1.4 GHz, 18.7 GHz and 36.5 GHz did not
 210 completely overlap, the measured results showed that the brightness temperatures observed ~~by~~
 211 radiometers at the left, middle and right of the orbit varied ~~less than within~~ 1 K. Therefore, the snow and
 soil ~~characteristics conditions~~ were considered homogeneous within the view fields of the three antennas.



212
213 **Figure 2. Ground-based microwave radiometer observation system.**
214

215 **2.2.2 Snow pit measurement**

216 The snow characteristics ~~were obtained by manual snow pit measurements in the black field,~~
217 including snow layering, snow layer thickness, grain size, snow density, and snow temperature, ~~were~~
218 collected by manual snow pit measurements in the black fields. These data were daily collected during
219 8:00-10:00 am local time, from November 27, 2015 to March 25, 2016, except 7 days (please see Table
220 3). Although the snow temperatures were manually measured at snow pits, the automatically collected
221 snow temperatures in the red field were utilized in this study, because the temperature measured at snow
222 pits could not reflect the natural temperature profile when the snow pits exposed to air.
223

224 **Table 3. Variables collected by manual daily snow pit measurement in black field in figure 1, ~~and~~ along with**
225 **their observation instruments, observation time and frequencies.**

Parameter	Instruments	Precision	Layering style	Observation time or frequency	Absent date
Layer thickness (cm)	Ruler	0.1cm	Natural layering	local time	no
Snow density (g/cm ³)	Snow tube (Chinese Meteorological Administration)	pressure: 0. 1g/cm ² , snow depth: 0.1 cm	Whole snowpack	8:00-10:00 am	no
Snow density (g/cm ³)	Snow shovel (NIEER)	weight: 0.01g, volume: 1cm ³	Every 10 cm		January 2-3, 2016;

Snow density (g/cm ³) and	Snow fork (Toikka Engineering Ltd.)	0.0001g/cm ³	Every 5 cm	February 20, 2016
Liquid water content (%)	Snow fork	0.001%	Every 5 cm	
Snow grain size (mm)	Anyty V500IR/UV	0.001mm	Natural layering	December 24, 31, 2015;
Snow grain shape	Shape card	N/A	Natural layering	January 1-3, 23, 2016, February 20, 2016

226

227

228

229

230

231

232

233

234

235

236

237

238

239

240

241

242

243

244

245

246

247

248

249

250

251

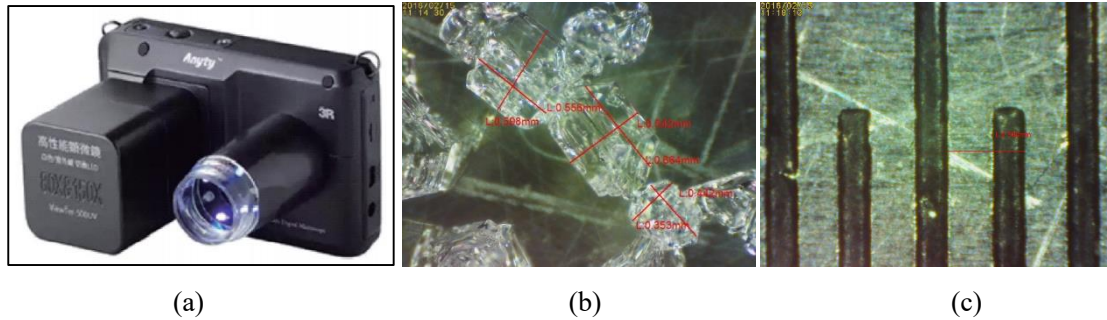
252

253

254

The first step of snow pit measurement is making a snow pit. In the black field, a new snow pit was dug each day ~~using a spade~~ ~~was used to excavate snow pit~~. The ~~length of the~~ snow pit ~~profile~~ was approximately 2 m x 1 m to make sure all parameters ~~could be~~ measured from unbroken snowpack. ~~The width of the snow pit was approximately 1 m.~~ The snow pit section was made as flat as possible using a flat shovel or ruler. When the snow profile is exposed to air for a long time, the snow characteristics will be influenced by environment and will be different from the natural snow characteristics. In order to make sure every observation conducted on natural snow pit, the snow pit was backfilled with the shoveled snow after finishing all observations, and the new snow pit in the following day was made at least 1-m distance ~~away~~ from the ~~last latest~~ snow pit. After finishing a snow pit, the natural snowpack stratification was then visually determined, and the thickness of each layer was ~~measured using~~ ~~recorded against~~ a ruler.

The ~~third next~~ step was measuring grain size and shape type in each layer. The grain size and type within each natural layer were estimated visually ~~from using~~ a microscope with an “Anyty V500IR/UV” camera (Figure 3a). ~~A~~ ~~The~~ software “VIEWTER Plus” ~~matched the microscope~~ was used to measure grain size. The grain type was determined based on Fierz et al. (2009). In this experiment, we utilized the length of longest axes and the length of shortest axes to describe grain size (Figure 3b). When using the software to measure the grain size, a reference must be needed. In this experiment, a ruler ~~with marked~~ 0.5 mm ~~marking~~ was used as a reference (Figure 3c). We adjusted the focus of the camera to make sure the grains at the clearest status in camera to take photos, and the photo of ruler scale was taken at the same focus. If the thickness of one layer was less than 10 cm, measurements were performed at the top and bottom of the layer, ~~respectively~~. If the thickness was greater than 10 cm, measurements were performed at the top, middle, and bottom of the layer, ~~respectively~~. For each layer, at least 5 photos were taken, and ~~the longest axes length and the shortest axes length of~~ at least 10 typical grains were ~~chosen to measure~~ ~~recorded~~ ~~the longest axes length and the shortest axes length in the photos of each layer.~~ ~~Each layer had at least 10 groups of longest and shortest axes length;~~ ~~the~~ final grain size was the average of ~~these values~~ ~~10-group recorded values~~. Figure A1 presents an example of the original photos of grains in each layer, and Table A1 shows the matched record of longest and shortest axis length.



255
256
257 **Figure 3-** (a) Picture of microscope “Anyty V500IR/UV” (a), (b) the measured longest axes lengths and
258 shortest axes length of particles (b), and (c) the reference ruler scale (c).

259
260 Snow density was measured using three instruments: snow tube, snow shovel and Snow-snow Fork
261 fork (Figure 4). The snow tube instrument, designed by Chinese Meteorological administration, contains
262 a metal tube with the base area of 100 cm² and the length of 60 cm, and a balance (figure 4a). It was
263 utilized to measure the snow density of a whole snowpack by weighing the snow sample. The snow
264 shovel is a 1500 cm³ wedge-type sampler, and its length, width and height are 20 cm, 15 cm, and 10 cm,
265 respectively (figure 4b). It was utilized to measure snow density every 10 cm (0-10 cm, 10-20 cm, 20-
266 30 cm...). The Snow-snow Fork-fork (figure 4c) is a microwave resonator that measures the complex
267 dielectric constant of snow, and adopts a semi-empirical equation to estimate snow density and liquid
268 water content based on the complex dielectric. The Snow Fork (figure 4e) was utilized to measure snow
269 density and liquid water content at 5-cm intervals starting 5 cm above the snow/soil interface (5cm, 10cm,
270 15 cm, 20cm...). In order to decrease the observation error, every measurement was conducted repeated
271 three times. If there is was an abnormal value, the a fourth measurement would be performed to make
272 sure ensure the accuracy. Table A2 is an example record table for snow density. The average value of the
273 three-time observation was the final value.



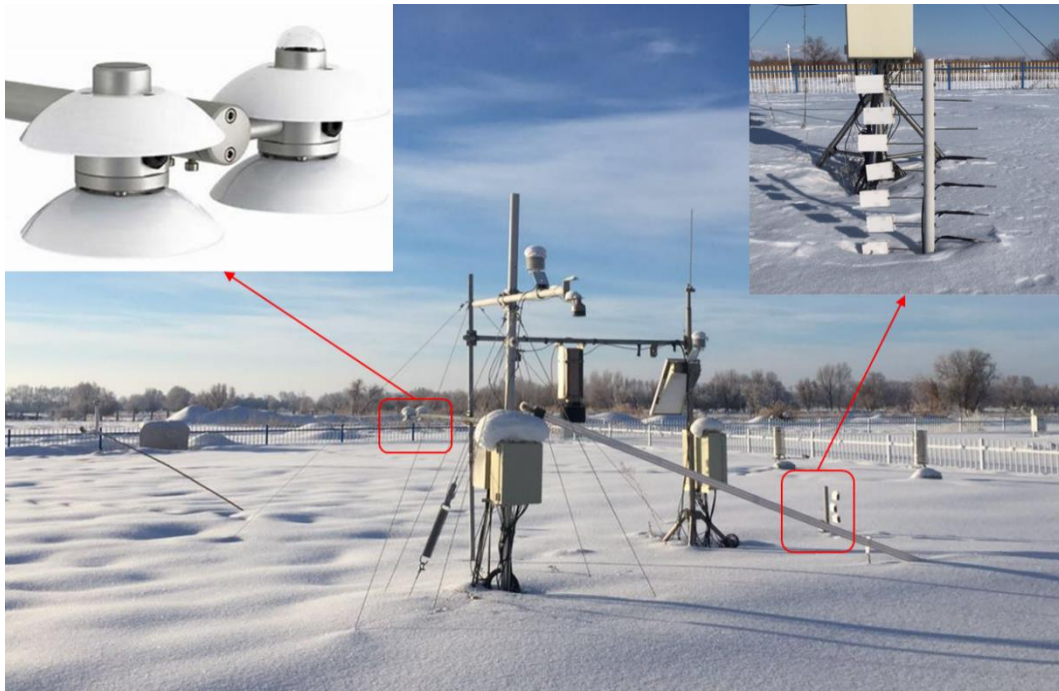
274
275
276
277 **Figure 4-** Three instruments for snow density: (a) Snow tube (a), (b) Snow shovel (b), and (c) Snow Fork
278 fork (c).

279 2.2.3 Automatic radiation and temperature measurement

280
281 In the red field, the 4-component radiation was automatically measured by Component Net
282 Radiometer (NR01) manufactured by Hukseflux, and layered snow temperatures was measured by
283 Campbell 109S temperature sensors, respectively. The temperature sensors were set up on a vertical pole

284 ~~which pole~~ ~~was vertically~~ inserted in ~~the~~ soil (Figure 5). The ~~heights of the~~ sensors' heights are 0 cm, 5
 285 cm, 10 cm, 15 cm, 25 cm, 35 cm, 45 cm, and 55 cm above soil/snow interface, ~~and temperatures were~~
 286 ~~collected data~~. ~~The snow temperatures at these heights were collected~~ every ten minute.

287 The NR01 net radiometer was set up to measure the energy balance between incoming short-wave
 288 and long-wave far infrared radiation versus surface-reflected short-wave and outgoing long-wave
 289 radiation. The range of short wave is 285~3000nm, and the range of long wave is 4.5~40 μ m. The 4-
 290 component radiation was automatically recorded every ten minutes. In addition, the sensor ~~is~~ ~~was~~
 291 equipped with a Pt100 temperature sensor for parallel recording of the sensor temperature.



292
 293 **Figure 5:** Set up of temperature sensors and CNR01 in the red field.

294
 295 **2.2.4 Meteorological observation**

296 The meteorological data include air temperature, air pressure and humidity, wind speed, soil
 297 temperature at -5 cm, -10 cm, -15 cm and -20 cm, and soil moisture at -10 cm and -20 cm. These
 298 parameters are routine observations conducted at ANRMS, ~~and were obtained through request from~~
 299 ~~ANRMS~~. The instruments used for soil and weather parameters observations are produced by China
 300 Huayun Meteorological Technology Group ~~corporation~~ Corporation. The measurement parameters and
 301 their measurement instruments are listed in table 4.

302 **Table 4. Automatically observed variables and the observation instruments, observation time and**
 303 **frequencies.**

Parameter	Instruments	Precision	Layering style	Observation time or frequency
Snow temperature(°C)	Temperature sensors (Campbell 109S)	0.001 °C	0 cm, 5 cm, 10 cm, 15 cm, 25 cm, 35 cm, 45 cm, and 55 cm	Ten-minute

4-component radiation (W/m^2)	Component Net Radiometer NR01 (Hukseflux)	$0.001 W/m^2$	6 feet above ground	Ten-minute
Soil temperature ($^{\circ}C$)	Soil temperature sensor (China Huayun)	$0.1^{\circ}C$	-5cm, -10 cm, -15cm and -20 cm	Hourly
Soil moisture (%)	Soil moisture sensor (DZN3, China Huayun)	0.1%	-10 cm and -20 cm	Hourly
Air temperature ($^{\circ}C$)	Thermometer screen (China Huayun)	$0.1^{\circ}C$	6 feet above ground	Hourly
Air pressure (hPa)	Thermometer screen (China Huayun)	0.1 hPa	6 feet above ground	Hourly
Air humidity (%)	Thermometer screen(China Huayun)	1%	6 feet above ground	Hourly
Wind speed (m/s)	Wind sensor(China Huayun)	0.1m/s	10 m above ground	Hourly

304

305

306

307

308

The air temperature, pressure and humidity were collected using temperature and wetness sensor in thermometer screen. The wind speed and direction were measured using wind sensor set up at 10 m on a tower. Soil moisture and temperature were automatically measured using moisture sensor and temperature sensor. Figure 6 depicts the instruments for these observations.

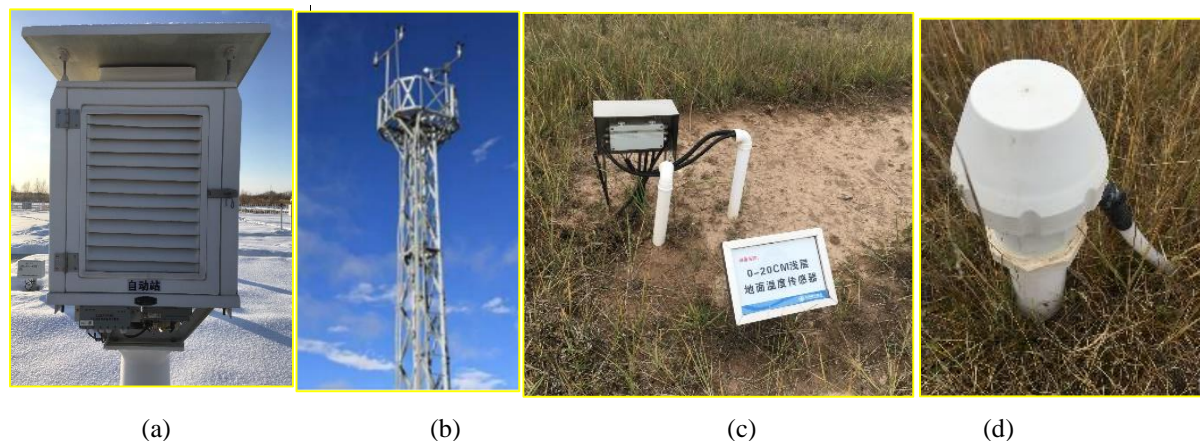


Figure 6: Instruments for observation of (a) air temperature and wetness (a), (b) wind speed (b), (c) soil temperature (c) and (d) soil moisture (d).

313

3 Description of consolidated IMCS dataset

314

315

316

317

318

319

320

The microwave brightness temperature, snow parameters, meteorological data were recorded in different formats, and their observation frequencies and times were different. These data must be reorganized and consolidated for ease of use. The values from the three-time measurements for snow density in each layer were averaged to obtain the final snow density. The length of the longest and shortest axes of particles in each photo were measured using the software. The average lengths of longest and shortest axes from all photos in each layer were obtained as the final grain size. The daily snow pit data were finally consolidated into a NetCDF file “snow pit data.nc”.

The time series of automated layered snow temperature and 4-component radiation data were first processed with-by removal of abnormal values and gap fill, and then were consolidated into a NetCDF file “ten-minute 4 component radiation and snow temperature.nc”. The ground-based brightness temperatures and the formatted weather and soil data requested from ANRMS were provided ‘as is’. Brightness temperature data were divided into time series of brightness temperature and multi-angle brightness temperatures, and separately stored in two NetCDF files, and the weather and soil data were consolidated into a NetCDF file “hourly meteorological and soil data.nc”. Table 3 describes the contents of the provided dataset.

1) Brightness temperatures data:

1-Minutely brightness temperature at 1.4 GHz, 18 GHz and 36 GHz for both polarizations at incidence angle of 50°. This data include date, time, incidence angle, azimuth angle, and brightness temperatures at the three bands for both polarizations.

2-Seventeen groups of calibrated brightness temperature at 1.4 GHz, 18.7 GHz and 36.5 GHz for both polarizations at different incidence angles (30, 35, 40, 45, 50, 55, 60°). This data include date, time, incidence angles, azimuth angle, and brightness temperatures at the three bands for both polarizations.

2) Manual snow pit data:

Daily snow pit data include date, snow depth, layered snow thickness, average longest axis, average shortest axis, grain shapes of each layer; layered snow density using snow fork (snow density at different heights, such as SF_5cm, SF_10cm, SF_15cm), snow density using snow tube, layered snow density using snow shovel (such as SS_0-10cm, SS_10-20cm, SS_20-30cm, SS_30-40cm).

3) Automated snow temperature and radiation data

Ten-minute 4-component radiation and snow temperature data include date, time, short-wave incident radiation, short-wave reflected radiation, long-wave infrared incident radiation, long-wave infrared reflected radiation, sensor temperature, and snow temperatures at different heights (such as ST_0cm, ST_5cm)

4) Meteorological and soil data:

Hourly weather data include date, hour, time, air temperature, pressure, humidity, wind speed, soil temperature at 5 cm, 10 cm, 15 cm and 20 cm, and soil moisture at 10 cm and 20 cm.

Table 3. Description of consolidated data

Data	Content	File name	Variables
Brightness temperature	Brightness temperature	TBdata.nc	Time (yyyy-mm-dd hh:mm:ss)Year, month, day, hour, minute, second , Tb1h, Tb1v, Tb18h, Tb18v, Tb36h, Tb36v, incidence angle, azimuth angle
	Multi-angle brightness temperatures	TBdata-multiangle.nc	Time (yyyy-mm-dd hh:mm:ss)Year, month, day, hour, minute, second , Tb1h, Tb1v, Tb18h, Tb18v, Tb36h, Tb36v, incidence angle, azimuth angle
Manual snow pit data	Layer thickness, layered grain size and shape, snow density	Daily snow pit data.nc	Time (yyyy-mm-dd)Year, month, day , snow depth, th1, Lg1, Sg1, th2, Lg2, Sg2, th3, Lg3, Sg3, th4, Lg4, Sg4, th5, Lg5, Sg5, th6, Lg6, Sg6, Stube, SS_0-10, SS_10-20, SS_20-30, SS_30-40, SS_40-50, SF_5, SF_10, SF_15, SF_20, SF_25, SF_30, SF_35, SF_40, SF_45, SF_50, shape1, shape2, shape3, shape4, shape5, shape5

Automated snow temperature and radiation data	4-component radiation, snow temperature	Ten-minute 4 component radiation and snow temperature.nc	<u>Time (yyyy-mm-dd hh:mm)</u> Year, month, day, hour, minute, SR_DOWN, SR_UP, LR_DOWN, LR_UP, T_Sensor, ST_0cm, ST_5cm, ST_15cm, ST_25cm, ST_35cm, ST_45cm, ST_55cm
Meteorological and soil data	meteorological data, soil moisture and temperature	Hourly meteorological and soil data.nc	<u>Time (yyyy-mm-dd hh)</u> Year, month, day, hour, Tair, Wair, Pair, Win, SM_10cm, SM_20cm, Tsoil_5cm, Tsoil_10cm, Tsoil_15 cm, Tsoil_20cm

351 Note: th: snow thickness, Lg: long axis, Sg: short axis, shape: grain shape;
352 Stube: snow density observed using snow tube, SS: snow density observed using snow shovel, SF: snow density
353 observed using snow fork; ST: snow temperature; SR_DOWN: downward short-wave radiation, SR_UP: upward
354 short-wave radiation, LR_DOWN, downward long-wave radiation, LR_UP: upward long-wave radiation, T_sensor:
355 sensor temperature; Tair: air temperature, Wair: air wetness, Pair: air pressure, Win: wind speed.

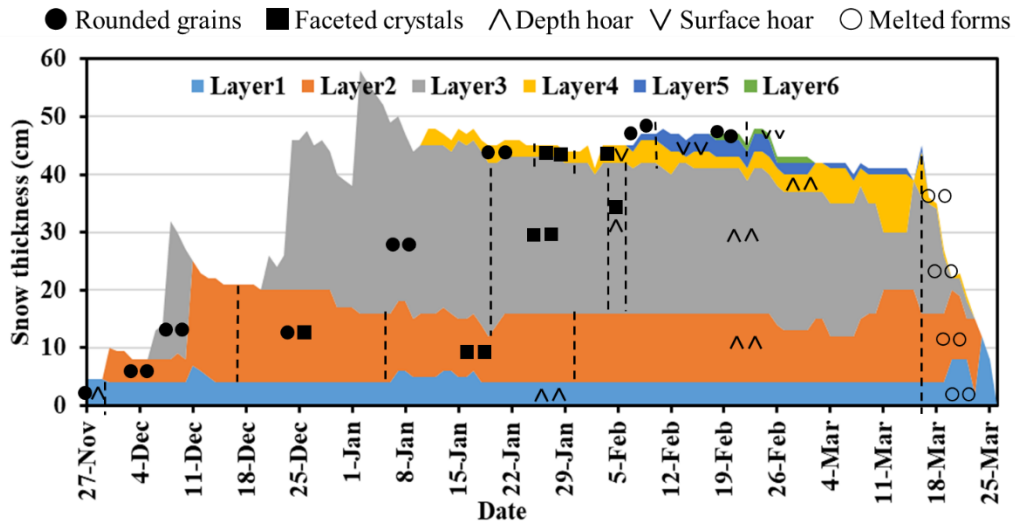
356 4 Overview and preliminary analysis of collected data from IMCS

357 4.1 Snow characteristics

358 4.1.1 Layering grain size and grain shape

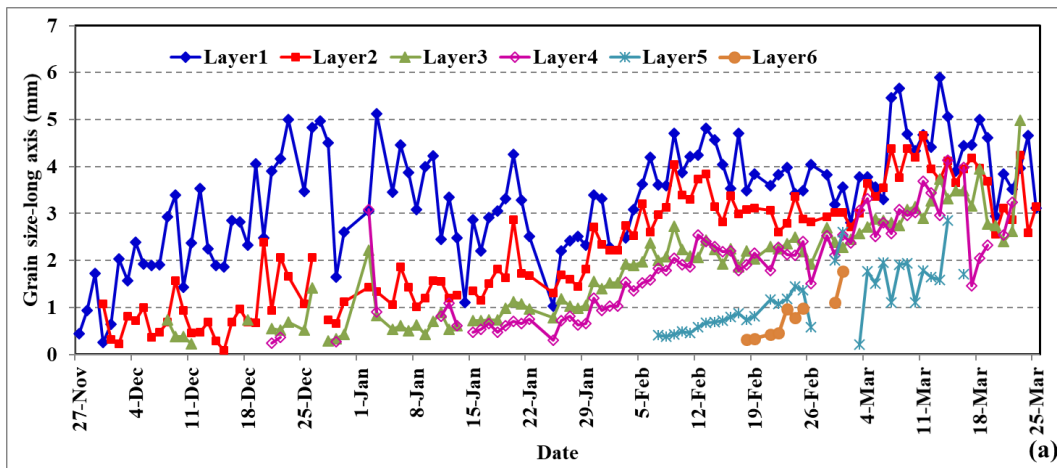
359 During 2015/2016, snow cover began on ~~25~~ November ~~25~~, of 2015, and ended on March 25, of
360 2016. During this snow season, there were seven snowfall events and each formed a distinct snow layer
361 except for the third event whose layering ~~became was~~ indistinguishable from the second layer (Figure 7
362 gray). The fourth event was the biggest, ~~After, after which time the~~ snow depth started to decrease and
363 ~~the~~ snow density increased. Snow cover began melting on March 14 and ~~snow depth declined to~~
364 ~~zero disappeared ended~~ within 10 days.

365 Grain sizes within all layers increased during the snow season, except in the bottom layer where
366 grain size experienced a decrease from December 28 to January 20 (Figure 8). In the vertical profile,
367 grain size increased from top to bottom with the snow age. The grain size of the fresh snow was
368 approximately 0.3 mm during the experiment. The biggest long and short axis, occurring in Layer 1 in
369 during the melt period, were up to 6 cm and 4 cm, respectively, ~~and occurred in Layer 1 in during the~~
370 ~~melt period~~. The length of short axes is approximately 0.7 of the length of long axes. The grain shape
371 generally developed from rounded grains to facet crystals, and then to depth hoar. After March 13, 2016,
372 the minimum air temperature increased to above 0°C, ~~snowpack melts snowmelt~~ accelerated, and the grain
373 shape developed to melted forms (Figure 7).

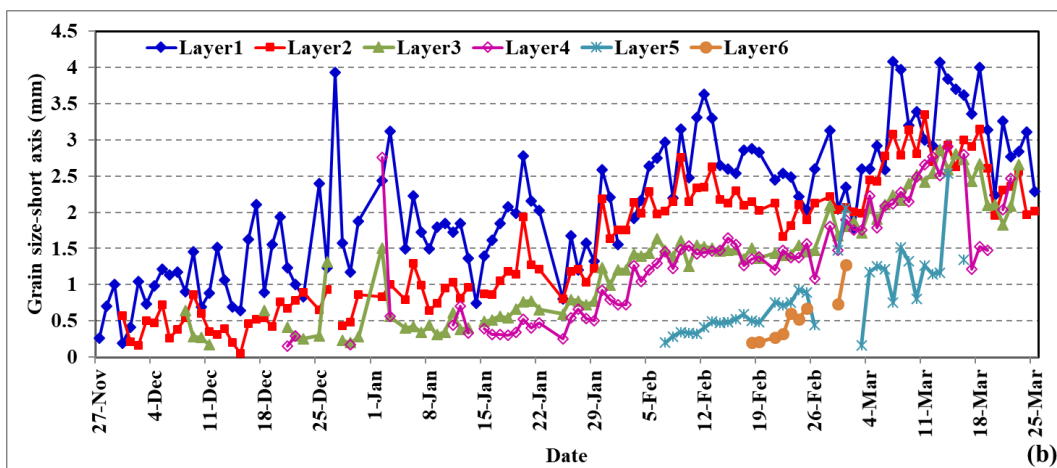


374

375 Figure 7: Daily variation in snow layers and grain shape in each layer from November 27, 2015 to March 25,
 376 2016.



377



378

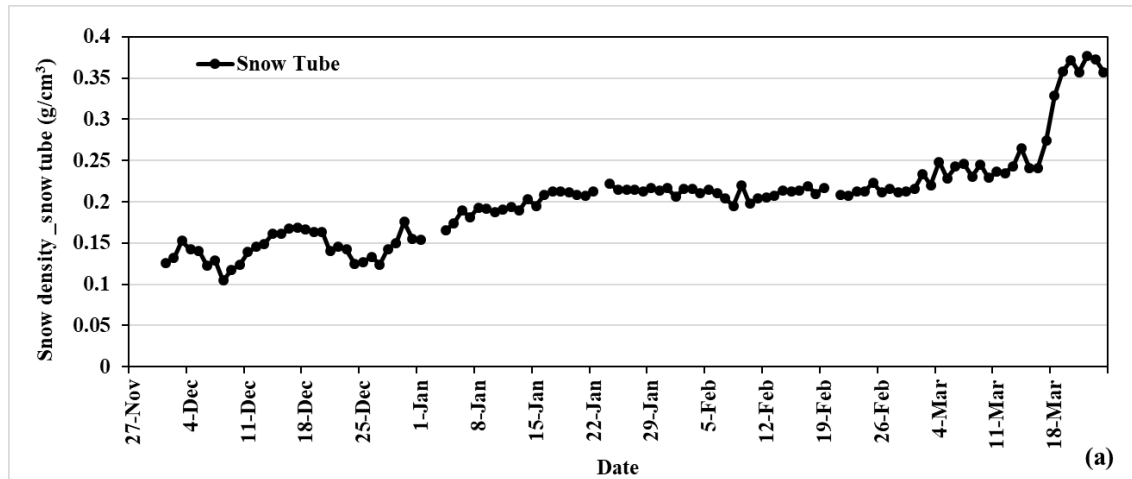
379 Figure 8: Daily variation in grain size within each layer from November 27, 2015 to March 25, 2016. The
 380 thickness of each layer/layer height/thicknesses are presented in figure 97.

381

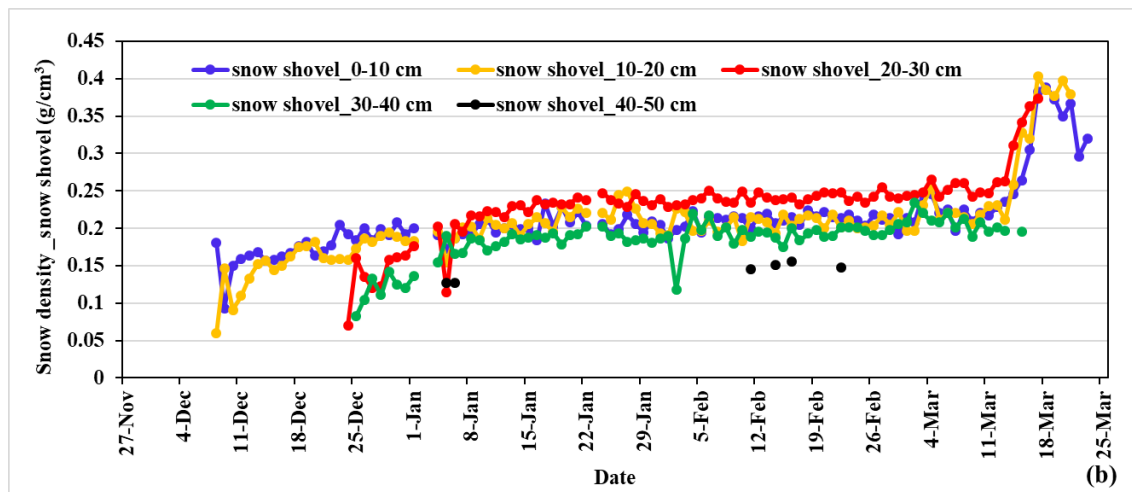
382 4.1.2 Snow density

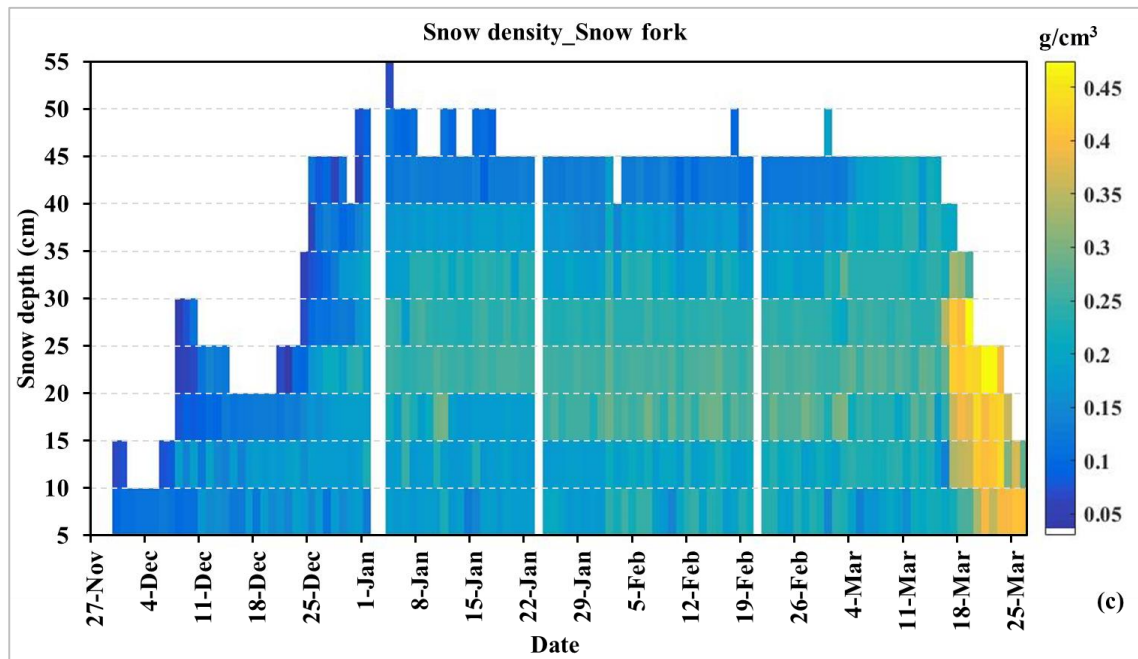
383 Snow densities measured by three different instruments shows that the density of fresh snow
 384 ranged between 0.05~1.0 g/cm³ (Figure 9). The snow densities increased with snow age, and remained
 385 stable after reaching ~0.2-0.25 g/cm³. From March 14 on, snow densities abruptly increased, ~~and with~~
 386 the maximum value ~~reached was~~ over 0.45 g/cm³. In the vertical profile, snow density increased from
 387 top to bottom in the accumulation phase. ~~However, but~~ after January 3, 2016, snow densities in the
 388 middle layers were larger than those in the bottom and upper layers due to the well-developed depth hoar
 389 of bottom layer. In the melting phase, ~~there were no significant different for the~~ snow densities in all
 390 layers ~~showed little difference~~. Snow fork provided most detail snow density profile, but ~~it~~ systematically
 391 underestimated snow density compared with snow tube and snow shovel by 24% (Dai et al., 2022).

392



393



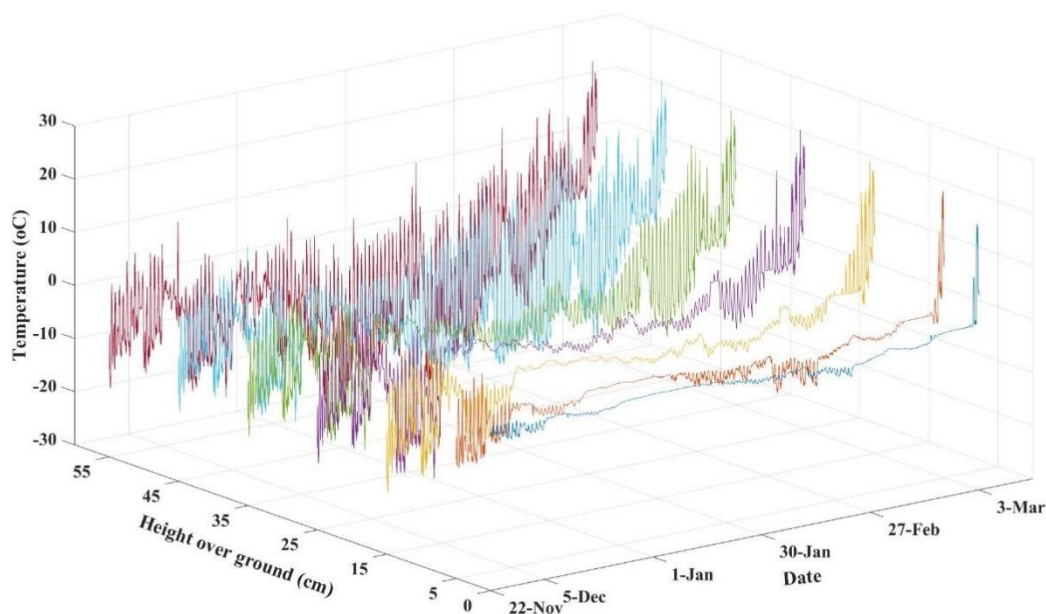


394
 395 Figure 9:- Daily variation in snow densities measured using three different measurement methods from
 396 November 27, 2015 to March 25, 2016. (a) overall snow density measured using snow tube, (b) snow density
 397 at 10-cm interval using snow shovel, and (c) snow density at 5-cm interval using snow fork.

398

399 **4.1.3 Snow temperature**

400 The diurnal range of snow temperature decreased from top to bottom layers. As and as the snow
 401 depth increased, there were more layers with small diurnal variations (Figure 10). Snow temperature at
 402 0 cm (snow/soil interface temperature) showed little-no significant diurnal variation, remaining at
 403 approximately -2.0 to 0.7 °C. Snow temperature in the top layer had the largest diurnal variation. The
 404 diurnal range decreased from top to bottom layers and as the snow depth increased there were more
 405 layers with small diurnal variations (Figure 10). After March 17, 2016, the snow temperature of all layers
 406 were over 0°C, which means implying that snow cover did not refreeze anymore.

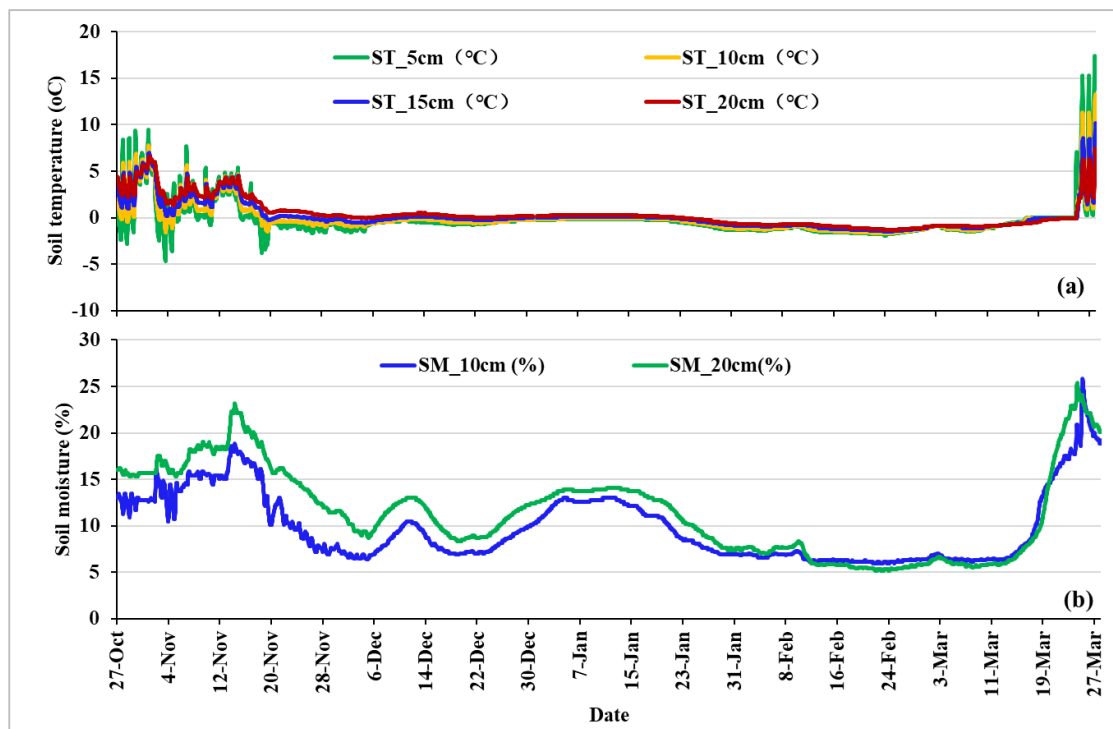


407

408 Figure 10: Minutely variation in layered-snow temperatures at 0 cm (snow/soil interface), 5 cm, 15 cm, 25
 409 cm, 35 cm, 45 cm and 55 cm above ground during experiment time-period

410 4.2 Soil temperature and moisture

411 The soil temperature at 5 and 10 cm remained stable and below 0 °C during the snow season but
 412 presented large fluctuation before (after) snow on (off) (Figure 11). The temperature difference between
 413 5 cm and 10 cm was much larger before snow cover onset than during snow cover period. The soil
 414 moistures at 10 cm were above 10% before snow cover onset and after snow off, and there were two
 415 soil moisture peaks within the snow cover period, one from December 12-14 and another the other from
 416 January 1-20, within the snow cover period.



417
 418 Figure 11: (a) Hourly soil temperature at 5 cm, 10 cm, 15 cm and 20 cm below the snow/soil interface (a),
 419 and (b) soil moisture at 10 cm and 20 cm below the snow/soil interface (b).

420 4.3 Brightness temperature

421 The microwave brightness temperatures varied with snow and soil characteristics, and weather
 422 conditions. Figure 12 shows the daily brightness temperatures, brightness temperature difference
 423 between 18 and 36 GHz, and snow depth at 1:00 am local time. Figure 13 shows the hourly variation in
 424 brightness temperatures at 1.4 GHz, 18.7 GHz and 36.5 GHz and air temperature after February 1. Data
 425 show that Tb36h and Tb36v decreased during the full snow season, Tb18h shows exhibited an obvious
 426 decline after February 18, and Tb18v after March 3 (Figure 12). After January 4, though snow depth
 427 stopped increasing, but the brightness temperature continued to decrease and brightness temperature
 428 difference increased. Based on Figure 8, snow density became stable on after January 15. Therefore, after
 429 January 4, the decreasing brightness temperatures was mainly caused by growing grain size. The
 430 variation of L band mainly relies on soil moisture and soil temperature change. We have soil temperatures

at 0 cm, 5 cm and 10 cm and soil moisture at 10 cm. However, the L band reflects the soil moisture within 5 cm which was absent in this experiment.

After February 25, brightness temperature exhibited a distinct cycle of daytime increase and nighttime decrease (Figure 13), resulting from large liquid water content caused by high daytime air temperature (above 0°C) and the melted snowpack refreezing at nighttime. After March 14, there was another big rise in air temperature and even the nighttime air temperatures were above 0°C. During this period of accelerated snowmelt, as the liquid water within the snowpack did not refreeze completely at night, and both the brightness temperatures at three bands and brightness temperature difference exhibited irregular behavior.

The variation of L band mainly rely on was mainly influenced by soil moisture and soil temperature change. We have soil temperatures at 0 cm, 5 cm and 10 cm and soil moisture at 10 cm. However, the L band reflects the soil moisture within 5 cm which was absent in this experiment. Actually, we did not find the variation of brightness temperature at L band had relationship with soil moisture at 10 cm and soil temperature.

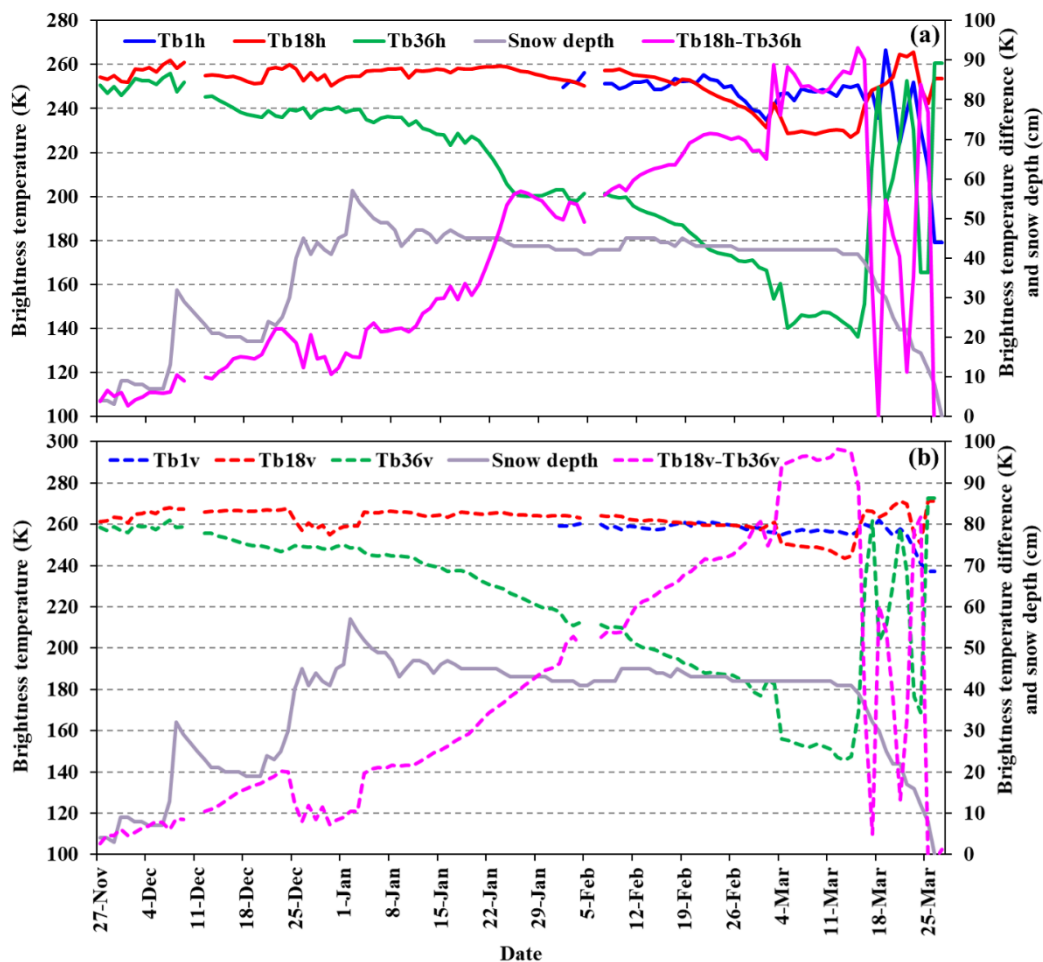
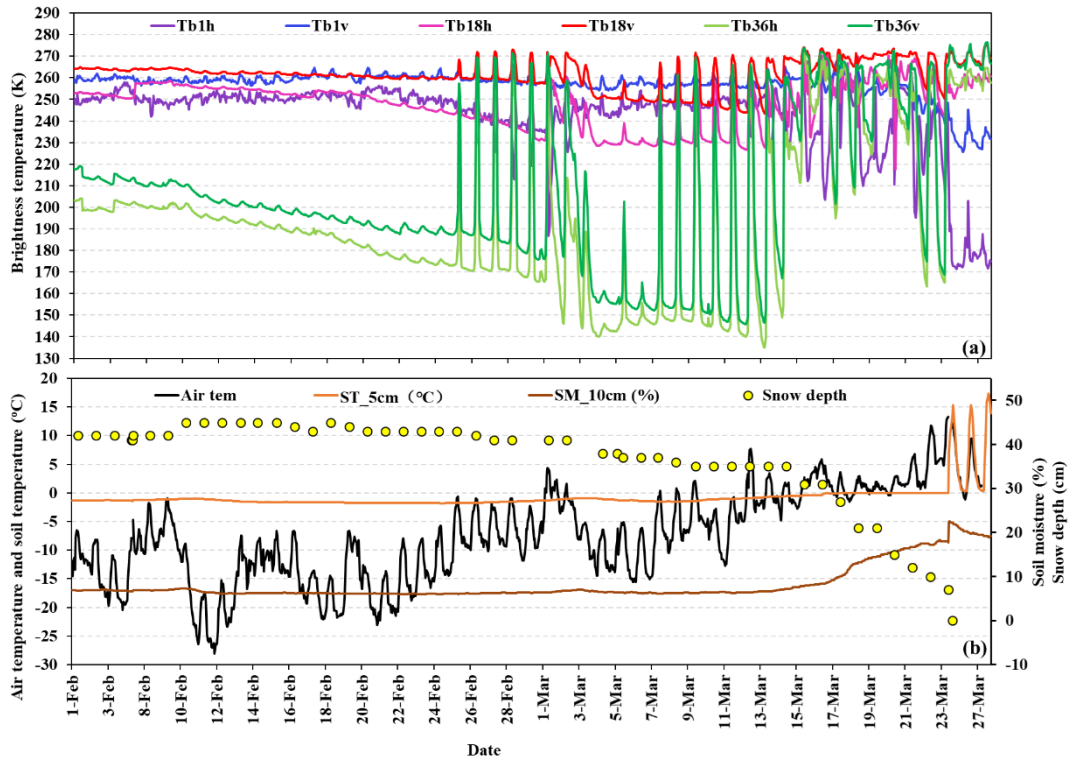


Figure 12: Daily variations in brightness temperatures at 1.4 GHz, 18 GHz and 36 GHz, for horizontal (Tb1h, Tb18h, Tb36h) and vertical polarizations (Tb1v, Tb18v, Tb36v), and the differences between Tb18h and Tb36h (Tb18h - Tb36h), and between Tb18v and Tb36v (Tb18v - Tb36v), at 1:00 am (local time), from November 27, 2015 to March 26, 2016. (a) for horizontal polarization, and (b) for vertical polarization.

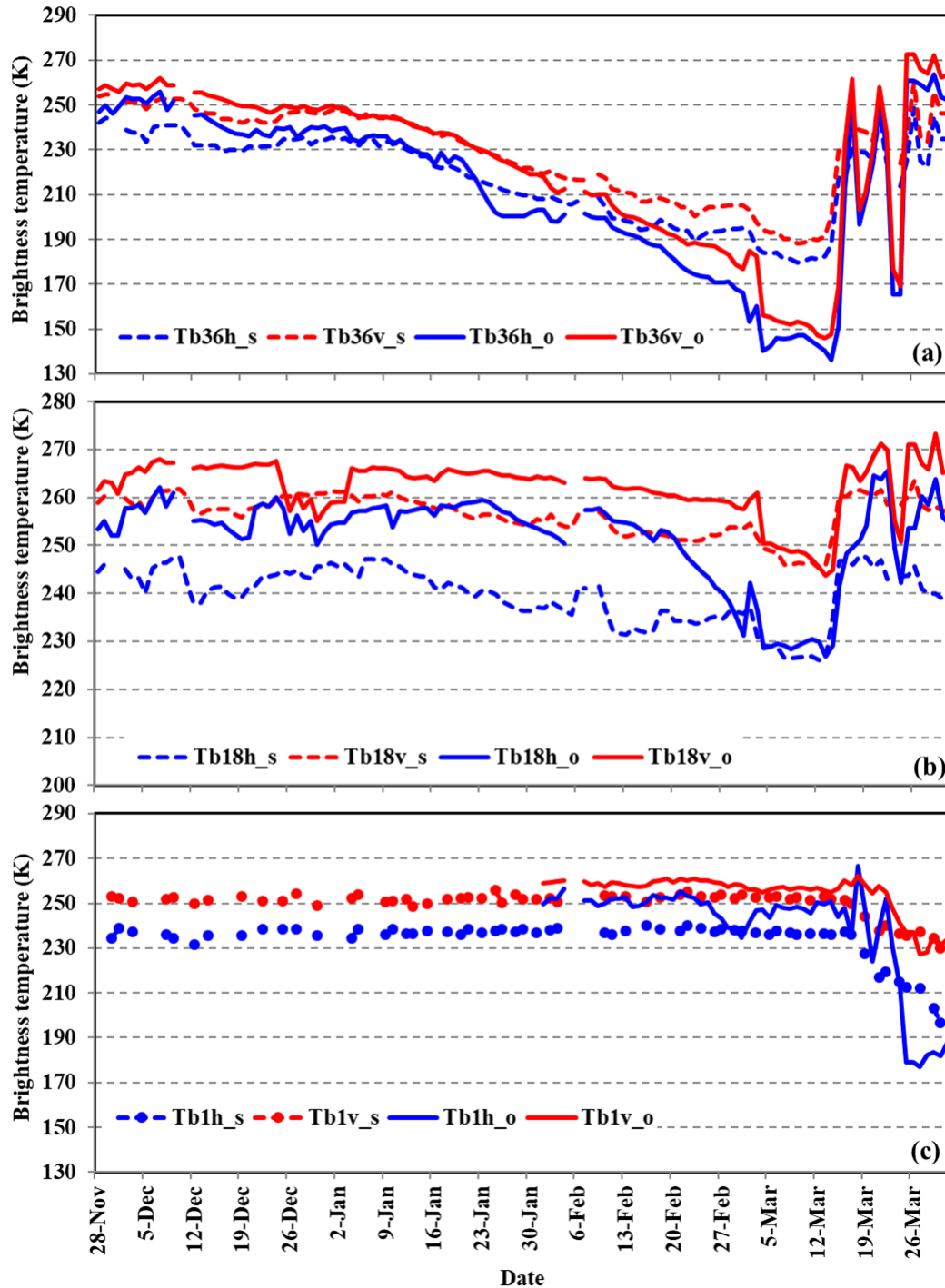
450
451



452
453 **Figure 13.** Hourly variation in (a) Tb1h, Tb18h, Tb36h, Tb1v, Tb18v, and Tb36v (a), and (b) air
454 temperature, soil moisture at 10 cm and soil temperature at 5 cm, and daily variation in snow depth (b),
455 from February 1 to March 28, 2016.

456

457 The brightness temperatures at 18.6–7 and 36.5 GHz from AMSR-2 and at 1.4 GHz from SMAP
458 were compared with the ground-based observations at the overpass time (Figure 14). Although there
459 were large differences between satellite and ground-based observations, the general temporal patterns
460 are the same. Specifically, even the abrupt changes at 18.7 and 36.5 GHz between on March
461 3 and March 4–16 is captured by both satellites and ground-based sensors. Brightness temperatures
462 at 1.4 GHz from both SMAP and ground microwave radiometer kept stable before March 16, after when,
463 brightness temperature rapidly decreased because of the increase of liquid water content soil moisture.
464 The correlation coefficients at both polarizations were approximately 0.96, 0.7 and 0.88 for 36.5 GHz,
465 18.6–7 GHz and 1.4 GHz, respectively. Satellite observed brightness temperature presented less decrease
466 trend than ground-based observation, and the difference at 36.5 GHz is larger than those at 18.6–7 and
467 1.4 GHz. Brightness temperatures at 1.4 GHz from both SMAP and ground microwave radiometer kept
468 stable before March 16, after when, brightness temperature rapidly decreased because of the increase of
469 liquid water content. The difference between ground-based and satellite observation might be attributed
470 to the different field of viewing areas.



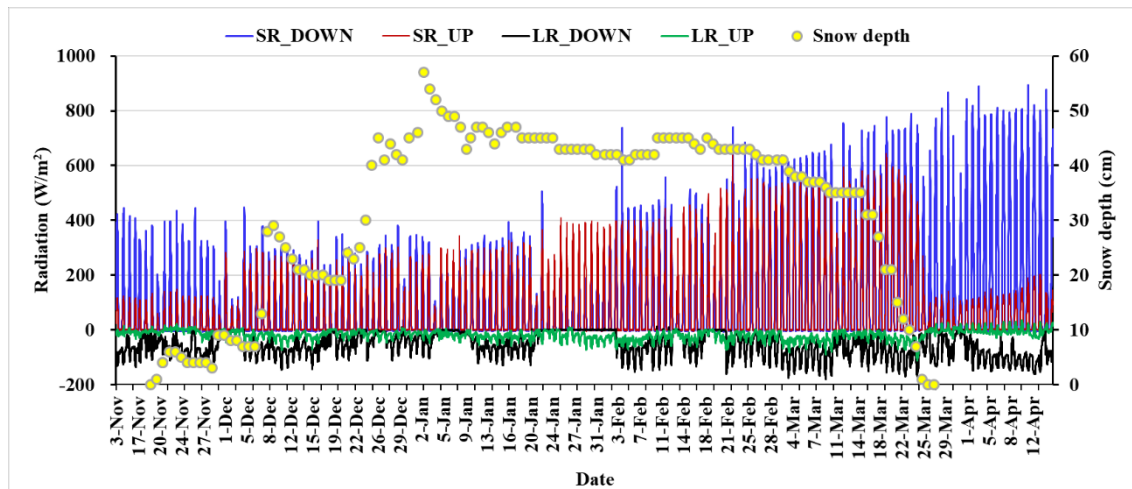
471

472 Figure 14: Comparison of brightness temperature between ground-based (o) and satellite-based
 473 observations (s: satellite; o: observation), (a) for 36 GHz, (b) for 18 GHz, and (c) for 1.4 GHz.

474 **4.4 4-component Radiation**

475 The land surface albedo is strongly related to the land cover. In this experiment, the downward
 476 short-wave radiation presented general increase after January, and while the trend became distinctive
 477 after February (Figure 15). The upward short-wave radiation abruptly increased when the ground was
 478 covered by snow (after November 21), and sharply declined on the snow off day (March 25). From the

479 first snowfall by the end of January, the ratios between upward and downward short-wave radiation were
 480 approximately 95%. The ratio decreased with snow age, and in the end of snow season, the ratios
 481 decreased to approximately below 50% on snow off day because of increasing melted water.



482
 483 **Figure 15:** Minutely variation in 4-component radiation and daily variation in snow depth at Altay station
 484 from November 3, 2015 to April 15, 2016.

485 5 Discussion

486 5.1 Applications

487 Although the Our dataset is, though just for one snow season observation, the provides daily snow
 488 pit observations with coincident microwave and optical radiation data, including comprehensive and in
 489 a full snow season provide the most detailed variation of snow parameters, which allowing researchers
 490 to find more details in snow characteristics and their relationship with remote sensing signatures. The
 491 dataset also fills the snow observation gap in mid-low snow depth area with relative short snow cover
 492 duration.

493 The snow pit data and microwave brightness temperatures have proven useful for evaluating and
 494 updating a microwave emission transfer model of snowpack (Dai et al., 2022). This dataset reflected the
 495 a general fact that brightness temperature at higher frequencies presented stronger volume scattering of
 496 snow grains, and were more sensitive to snow characteristics. This experiment revealed that the dominant
 497 control for the variation of brightness temperature was the variation of grain size but not the snow depth
 498 or SWE. In the stable period, The largest snow depth or SWE did not correspond to the largest brightness
 499 temperature difference between 18.7 and 36.5 GHz, in the condition of dry snowpack. Due to the growth
 500 of grain size, the maximum difference occurred by was increasing increased with growing grain size in the
 501 condition of dry snowpack before melting for stable snow cover. Therefore, the daily snow depth variations
 502 curve derived from passive microwave remote sensing datasets tend to exhibit a temporal offset from
 503 those of in situ observation.

504 During the snow season, brightness temperatures for both polarizations presented similar variation
 505 trends, but they though behaved behaving different in some time periods fluctuation. The horizontal
 506 polarization was more sensitive to environment and was less stable than vertical polarization. Besides,
 507 the polarization difference at 18.7 GHz and 36.5 GHz showed increase and decrease trends, respectively,
 508 during the experimental period. The This phenomenon was different from results for 18 GHz were
 509 opposite to the simulation results (Dai et al., 2022). The different polarization behavior at 18.7 and 36.5

510 GHz might be related to the environmental conditions, snow characteristics and soil conditions. However,
511 ~~as~~ the subsurface soil moisture was not observed, the dynamic ground emissivity could not be estimated.
512 ~~As it is known, as~~ L band has strong penetrability, ~~and~~ the brightness temperature variations were
513 predominantly related to subsurface soil conditions, ~~except when~~ unless for the situations that the liquid
514 water content within snowpack was high. Therefore, in the condition of soil moisture data absence, L
515 band brightness temperatures were expected to reflect soil moisture variation ~~which that~~ influences the
516 soil transmissivity (Babaeian et al., 2019; Naderpour et al., 2017; Hirahara et al., 2020).

517 Snow surface albedo significantly influences the incoming solar radiation, playing an important role
518 in the climate system. The factors altering snow surface albedo contains the snow characteristics (grain
519 size, SWE, liquid water content, impurities, surface temperature etc), external atmospheric condition and
520 solar zenith angle (Aoki et al., 2003). Snow albedo was estimated based on snow surface temperatures
521 in some models (Roesch et al., 1999), while others considered ~~that~~ snow surface albedo was mainly
522 related to to depend mainly on snow aging age (Mabuchi et al., 1997). In this experiment, we obtained
523 the 4-component radiation, snow pit and meteorological data. ~~These data provide~~ ing nearly all
524 observations of possible influence factors, ~~and therefore~~ could be utilized to ~~discuss and~~ analyze
525 shortwave radiation process of snowpack, and validate or improve multiple-snow-layer albedo models.

526 Snow grain sizes and snow densities within different layers presented different growth rates during
527 different ~~time periods~~ periods. Generally, the growth rates are related to the air temperature, pressure and
528 snow depth (Chen et al., 2020; Essery, 2015; Vionnet et al., 2012; Lehning et al., 2002); therefore, this
529 dataset can be used to analyze the evolution process of snow characteristics, as well as validation data
530 for snow models.

531 5.2 Uncertainties

532 During the experiment, some uncertainties were produced due to irresistible factors. It ~~is was~~
533 reported that the sampling depth of the L-band microwave emission under frozen and thawed soil
534 conditions is determined at 2.5 cm (Zheng et al., 2019). We did not collect subsurface soil moisture, and
535 the L band radiometer observation began on January 30, 2016. Therefore, it is difficult to obtain the
536 ground emissivity in the full snow season based on the data. The soil moisture data at 10 and 20 cm under
537 soil/snow interface cannot be directly used to validate and develop soil moisture retrieval from L band
538 brightness temperature. ~~We hope~~ In the future, detailed soil moisture profile will be observed to estimate
539 the subsurface soil moisture to fill the gap.

540 The grain size data were collected through taking photos. When measuring the length of grains, the
541 grain selection has subjectivity, and the released data are ~~average values~~ statistic results based on the
542 ~~chosen~~ recorded grain sizes. Although the general variation trend can be reflected by the time series of
543 average grain size, some details might be missed. Therefore, for who with interests, the original grain
544 photos could be provided through requesting for authors. In snow-melt period, large liquid water content
545 would influence the measurement results of snow fork. ~~So~~ Therefore, it is suggested to use small-size
546 snow shovel or cutter to observe layered snow density in future experiments.

547 One season observation is quite valuable for developing and validate remote sensing snow retrieval
548 method—or snow model, although the representativeness of this observation ~~remains unknown~~ requires
549 further analysis. ~~Nevertheless~~, We need more years of observations should be considered to increase the
550 statistical significance of to endorse or confirm the evolution of snow characteristics.

551 6 Conclusions

552 In a summary, the IMCS campaign provides ~~a time series of~~ snow pits observation, meteorological
553 parameters, optical radiation and passive microwave brightness temperatures in ~~the the~~ snow season of
554 2015/2016. The dataset is unique in providing microwave brightness temperatures and coincident daily
555 snow pits data over a full snow season at a fix site. The first use of our dataset is for the validation of
556 snow microwave emission models, improving its simulation accuracy.

557 The daily snow pit data ~~which provide a detail description of~~ snow grain size, grain shape, snow
558 density and snow temperature profiles. Generally, grain size grew with snow age, and increased from top
559 to bottom. Snow grains are rounded shape with small grain size in the top layer, and depth hoar with
560 large grain size in the bottom layer. Snow density experienced increase-stable-increase variation, and the
561 densities of the middle layers were greater than the bottom layer due to the well-developed depth hoar in
562 the stable period. The data can be used to analyze~~s~~ the evolution process of snow characteristics
563 combining with weather data, also for the validation and improve~~ment of~~ the snow process models, such
564 as SNOWPACK (Lehning et al., 2002), SNTHERM (Chen et al., 2020), etc. The improvement of these
565 snow process models can further enhance the prediction accuracy of land surface process and hydrology
566 models, ~~and the simulation accuracy of snow microwave emission models.~~

567 Microwave radiometer data and snow pit data have been utilized to analyze the volume scattering
568 features of snow-pack at different frequencies (Dai et al., 2022). Results showed that grain size ~~is was~~
569 the most important factor to influence snow volume scattering. The data can also be used ~~to for analysis~~
570 of further analyze polarization characteristics of snow-pack, combining with soil and weather data, ~~and~~
571 ~~be used to validate different microwave emission models of snowpack.~~

572 The microwave and optical radiations were simultaneously observed. Existing studies reported that
573 the optical equivalent diameter must be used in microwave emission model with caution (LöweLowe
574 and Picard, 2015; Roy et al., 2013). These data provide a good new opportunity to analyze the difference
575 between the influence of grain size on microwave and optical radiation, establishing the bridge between
576 effective optical grain size and microwave grain size.

577 7 Data availability

578 The IMCS consolidated datasets are available ~~after registration~~ on the National Tibetan Plateau Data
579 Center and available online at [http://data.tpdc.ac.cn/zh-hans/data/df1b5edb-daf7-421f-b326-](http://data.tpdc.ac.cn/zh-hans/data/df1b5edb-daf7-421f-b326-cdb278547eb5/)
580 [cdb278547eb5/](http://data.tpdc.ac.cn/zh-hans/data/df1b5edb-daf7-421f-b326-cdb278547eb5/) (doi: 10.11888/Snow.tpdc.270886). Microwave radiometry raw Data are available for
581 scientific use on request from Northwest Institute of Eco-Environment and Resources, Chinese Academy
582 of Sciences.

583

584

585 **Author contributions:** LD and TC designed the experiment. LD, YZ, JT, MA, LX, SZ, YY YH and LX
586 collected the passive microwave and snow pit data. HL provided the 4-component radiation and snow
587 temperature data. LW provided meteorological data. LD write the manuscript, and TC made revision. All
588 authors contributed to the data consolidation.

589

590 **Competing interests:** The authors declare that they have no conflict of interest.

591

592 **Acknowledgment:** The authors would like to thank the Altay meteorological station for providing
593 logistics service and meteorological data.

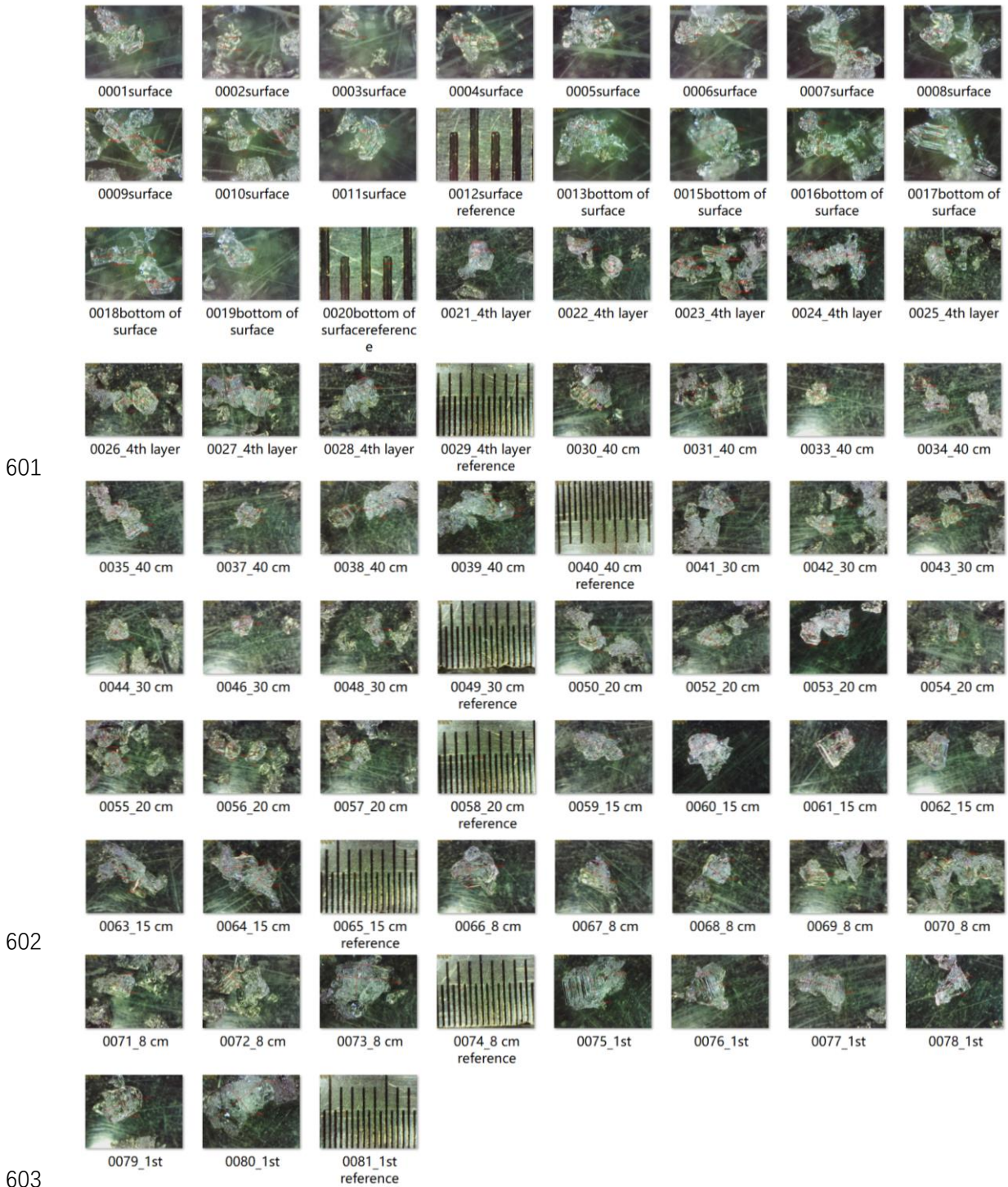
594

595 **Financial support:** This research was funded by the National Science Fund for Distinguished Young
596 Scholars (grant nos: 42125604), National Natural Science Foundation of China (grant nos: 42171143),
597 and CAS 'Light of West China' Program.

598

599

600 Appendix



601

602

603

604

605 Figure A1. Photos of grains and reference ruler in each layer on February 15, 2016. In, and in each photo

606 the longest and shortest axis lengths of the chosen grains are labeled. Original photos are in URL:

607 <http://arcticroute.tpsc.ac.cn/navigate/bmp>

608

609

610

611

612

Table A1. Recorded longest and shortest axis length in Figure A.

Stratigraphy	Thickness (cm)	Shape	Grain size (longest axis * shortest axis)(mm)								
the fifth	3cm	#22	0.595 *0.43 6	0.472 *0.47 1	0.450 *0.43 6	0.615 *0.47 4	0.374 *0.31 4	0.647 *0.30 7	0.656 *0.52 9	0.544 *0.51 9	0.717 *0.44 7
			0.750 *0.44 5	1.056 *0.95 5	0.623 *0.37 8	0.451 *0.40 5	1.397 *0.63 5	1.235 *0.32 7	0.600 *0.42 1	0.633 *0.55 6	0.729 *0.42 3
the fourth	3cm	#37	2.605 *2.01 1	1.850 *1.32 8	1.626 *1.55 4	1.767 *1.68 5	1.718 *1.53 5	2.255 *1.29 6	1.674 *1.60 1	1.542 *1.26 9	3.505 *1.44 0
			3.055 *1.77 4	1.448 *1.37	2.461 *1.91 4	2.757 *2.11 5	2.179 *2.05 9	2.393 *1.78 8			
the third	25cm	#27, #31, #37	2.569 *1.60 7	2.073 *2.13 0	2.591 *1.41 4	1.869 *1.80 2	2.067 *1.26 6	1.209 *1.10 6	1.719 *1.18 8	1.648 *0.97 5	1.911 *1.58 2
			1.921 *1.71 0	1.518 *1.06 7	1.291 *1.14 7	1.690 *1.55 1	1.756 *1.39 8	1.812 *1.26 3	1.733 *1.67 2	1.880 *1.51 8	2.411 *1.22 0
			2.118 *1.72 7	1.614 *1.45 7	1.795 *1.70 5	2.215 *2.31 1	1.864 *1.69 2	1.967 *1.65 1	2.008 *1.39 5	1.362 *1.14 1	1.484 *1.29 1
the second	12	#33, #34	4.251 *2.26 6	3.012 *2.65	2.805 *1.99 5	1.799 *1.41 5	1.402 *1.19 5	3.040 *2.07 3	2.850 *2.09 5		
			3.900 *2.53 2	2.420 *2.33 3	2.515 *2.20 6	2.044 *2.03 2	2.506 *2.36 3	2.894 *2.16 1	2.413 *1.95 0	2.494 *1.81 6	4.929 *3.25 7
the first	4	#40, #34, #38	4.933 *3.37 8	3.207 *2.77 4	3.562 *1.70 1	2.818 *1.66 8	3.581 *2.51 8	6.179 *3.56 2			

613

614

615

616

617

618

619
620
621

Table A2: ~~One~~ An example of record table for snow density observation.

observation date: 20160111		observation time: 9:03-9:40		weather: clear		snow depth: 48cm	
Snow Fork table				Snow tube table			
observation height (cm)	liquid water content(%)	snow density (g/cm3)	snow depth(cm)	46.5	47	47.5	
5	0	0.1923	snow pressure(g/cm2)	9.1	9	9.5	
	0.118	0.1882	snow density(g/cm3)	0.1957	0.1915	0.2000	
	0	0.1882					
10	0.461	0.164					
	0.46	0.1631					
	0.461	0.1361					
15	0.123	0.2532	snow shovel table				
	0	0.2506	observation layer (cm)	weight of shovel+snow(g)	weight of shovel(g)	snow density(g/cm3)	
	0	0.2417	0-10	865.04	572.16	0.1953	
0.24	0.2159	858.72		572.16	0.1910		
0.119	0.2155	866.69		572.16	0.1964		
20	0.119	0.2146	10-20	878.58	572.16	0.2043	
	0.117	0.1977		887.04	572.16	0.2099	
	0	0.1994		872.79	572.16	0.2004	
25	0	0.1984	20-30	905.34	572.16	0.2221	
	0	0.1919		903.41	572.16	0.2208	
	0	0.1966		907.88	572.16	0.2238	
30	0	0.1928	30-40	832.75	572.16	0.1737	
	0	0.1534		838.14	572.16	0.1773	
	0	0.1517		837.27	572.16	0.1767	
35	0	0.1472	40-50				
	0.325	0.1097					
	0	0.1054					
40	0.107	0.1088	50-60				
	0	0.0922					
	0	0.0991					
45	0	0.0928					
50							

622
623
624

625 **References:**

626 Aoki, T., Hachikubo, A., and Hori, M.: Effects of snow physical parameters on shortwave broadband
627 albedos, J. Geophys. Res-Atmos., 108 (D19), 4616, <https://doi.org/10.1029/2003JD003506>, 2003.
628 Babaeian, E., Sadeghi, M., Jones, S.B., Montzka, C., Vereecken, H., and Tuller, M.: Ground, Proximal,
629 and Satellite Remote Sensing of Soil Moisture-~~r~~, Reviews of Geophysics, 57(2), 530-616,
630 [https://doi.org/doi: 10.1029/2018RG000618](https://doi.org/doi:10.1029/2018RG000618), 2019.
631 Barnett, T.P., Adam, J.C., and Lettenmaier, D.P.: Potential impacts of a warming climate on water
632 availability in snow dominated regions. Nature, 438, 303-309, doi: 10.1038/nature04141, 2005.
633 Brucker, L., Hiemstra, C., Marshall, H.-P., Elder, K., De Roo, R., Mousavi, M., Bliven, F., Peterson,
634 W., Deems, J., Gadowski, P., Gelvin, A., Spaete, L., Barnhart, T., Brandt, T., Burkhardt, J., Crawford,
635 C., Datta, T., Erikstrod, H., Glenn, N., Hale, K., Holben, B., Houser, P., Jennings, K., Kelly, R., Kraft,
636 J., Langlois, A., McGrath, D., Merriman, C., Molotch, N., Nolin, A., Polashenski, C., Raleigh, M.,
637 Rittger, K., Rodriguez, C., Roy, A., Skiles, M., Small, E., Tedesco, M., Tennant, C., Thompson, A.,
638 Tian, L., Uhlmann, Z., Webb, R., and Wingo, M., and Jeon: A first overview of snowex ground-based
639 remote sensing activities during the winter 2016-2017. FIRST OVERVIEW OF SNOWEX GROUND-
640 BASED REMOTE SENSING ACTIVITIES DURING THE WINTER 2016-2017. Int. Geosci. Remote
641 Sen., 1391-1394 2017 Ieee International Geoscience and Remote Sensing Symposium (pp. 1391-1394),
642 <http://dx.doi.org/10.1109/IGARSS.2017.8127223>, 2017.
643
644 Che, T., Dai, L.Y., Zheng, X.M., Li, X.F., and Zhao, K.: Estimation of snow depth from passive-
645 microwave brightness temperature data in forest regions of northeast China. Remote Sensing of
646 Environment, 183, 334-349, doi: 10.1016/j.rse.2016.06.005, 2016.

647 ~~Che, T., Li, X., Jin, R., Armstrong, and R., Zhang, T.J.: Snow depth derived from passive microwave~~
648 ~~remote sensing data in China. *Annals of Glaciology*, 49, 145. doi: 10.3189/172756408787814690,~~
649 ~~2008.~~

650 Chen, T., Pan, J.M., Chang, S.L., Xiong, C., Shi, J.C., Liu, M.Y., Che, T., Wang, L.F., and Liu, H.R.:
651 Validation of the SNTherm Model Applied for ~~Snow-snow Depthdepth~~, ~~Grain-grain Sizesize~~, and
652 ~~Brightness-brightness Temperature-temperature Simulation-simulation~~ at ~~Meteorological-~~
653 ~~meteorological Stations-stations~~ in China-. *Remote SensingSens.*, 12, 507, <https://doi.org/doi>- Artn
654 50710.3390/Rs12030507, 2020.

655 Cline, D., Elder, K., Davis, B., Hardy, J., Liston, G., Imel, D., Yueh, S., Gasiewski, A., Koh, G.,
656 Armstrong, R., and Parsons, M.: An overview of the NASA Cold Land Processes Field Experiment
657 (CLPX-2002)-. *P. Soc. Photo-Opt. Ins. Microwave Remote Sensing of the Atmosphere and-*
658 *Environment Iii*, 4894, 361-372-, <https://doi.org/doi>: ~~Doi~~ 10.1117/12.467766, 2003.

659 ~~Cohen, J: Snow cover and climate. *Weather*, 49, 150-156, 1994.~~

660 Dai, L. (2020): Microwave radiometry experiment data in Altay (2015/2016)-. National Tibetan
661 Plateau Data Center [dataset]-. <https://doi.org/doi>: 10.11888/Snow.tpd.270886, 2020.

662 ~~Dai, L.Y., Che, T., Wang, J., and Zhang, P.: Snow depth and snow water equivalent estimation from-~~
663 ~~AMSR-E data based on a priori snow characteristics in Xinjiang, China. *Remote Sensing of-*~~
664 ~~*Environment*, 127, 14-29. doi: 10.1016/j.rse.2011.08.029, 2012.~~

665 ~~Dai, L.Y., Che, T.: Estimating snow depth or snow water equivalent from space. *Sciences in Cold and-*~~
666 ~~*Arid Regions*, 14(2): 1-12. doi: 10.3724/SP.J.1226.2022.21046, 2022.~~

667 Dai, L.Y., Che, T., Xiao, L., Akynbekkyzy, M., Zhao, K., and ~~LeppänenLeppanen~~, L.: Improving the
668 Snow Volume Scattering Algorithm in a Microwave Forward Model by Using Ground-Based Remote
669 Sensing Snow Observations-. *Ieee T. Geosci. Remote.Ieee Transactions on Geoscience and Remote-*
670 *Sensing*, 60-, 4300617-, <https://doi.org/doi>: 10.1109/TGRS.2021.3064309, 2022.

671 Derksen, C., Toose, P., Lemmetyinen, J., Pulliainen, J., Langlois, A., Rutter, N., and Fuller, M.C.:
672 Evaluation of passive microwave brightness temperature simulations and snow water equivalent
673 retrievals through a winter season-. *Remote Sens. Environ.Remote Sensing of Environment*, 117, 236-
674 248, <https://doi.org/doi>: 10.1016/j.rse.2011.09.021, 2012.

675 ~~Ding, Y.J., Yang, J.P., Wang, S.X., and Chang, Y.P.: A review of the interaction between the-~~
676 ~~cryosphere and atmosphere. *Sciences in Cold and Arid Regions*, 12 (6): 329-342, doi:-~~
677 ~~10.3724/SP.J.1226.2020.00329, 2020.~~

678 Essery, R.: A factorial snowpack model (FSM 1.0)-. *Geosci. Model Dev.* 2015-, 8, 3867-3876-.
679 <https://doi.org/10.5194/gmd-8-3867-2015>, 2015.

680 ~~Fierz, C., Armstrong, R.L., Durand, Y., Etchevers, P., Greene, E., McClung, D.M., Nishimura, K.,~~
681 ~~Satyawali, P.K. and Sokratov, S.A.: The International Classification for Seasonal Snow on the Ground.~~
682 ~~*IHP-VII Technical Documents in Hydrology N°83, IACS Contribution N°1, UNESCO-IHP, Paris,*~~
683 ~~2009.~~

684 Hirahara, Y., de Rosnay, P., and Arduini, G.: Evaluation of a ~~Microwave-microwave E~~missivity
685 ~~M~~odule for ~~S~~snow ~~c~~Covered ~~A~~Area with CMEM in the ECMWF Integrated Forecasting System-.
686 *Remote SensingSens.*, 12(18), doi: Artn 294610.3390/Rs12182946, 2020-<https://doi.org/>
687 [10.3390/rs12182946](https://doi.org/10.3390/rs12182946), 2020.

688 Immerzeel, W.W., van Beek, L.P.H., and Bierkens, M.F.P.: Climate Change Will Affect the Asian
689 Water Towers-. *Science*, 328(5984), 1382-1385-, <https://doi.org/doi>: 10.1126/science.1183188, 2010.

690 ~~Jiang, L.M., Wang, P., Zhang, L.X., Yang, H., and Yang, J.T.: Improvement of snow depth retrieval for~~

691 ~~FY3B MWRI in China. *Science China Earth Sciences*, 57, 1278–1292, doi: 10.1007/s11430-013-4798-~~
692 ~~8, 2014.~~

693 ~~Jordan, R.E.: A One-Dimensional Temperature Model for a Snow Cover. Technical~~
694 ~~Documentation for SNTherm.89; U.S. Army Cold Regions Research and Engineering Laboratory-~~
695 ~~Hanover, NH, USA, 1991.~~

696 ~~Lehning, M., Bartelt, P., Brown, B., Fierz, C., and Satyawali, P.: A physical SNOWPACK model for the~~
697 ~~Swiss avalanche warning Part II: Snow microstructure-, *Cold Reg. Sci. Technol. Cold Regions*~~
698 ~~*Science and Technology*, 35, 147–167, [https://doi.org/doi:10.1016/S0165-232x\(02\)00073-3](https://doi.org/doi:10.1016/S0165-232x(02)00073-3), 2002.~~

699 ~~Lemmetyinen, J., Kontu, A., Pulliainen, J., Vehvilainen, J., Rautiainen, K., Wiesmann, A., Matzler, C.,~~
700 ~~Werner, C., Rott, H., Nagler, T., Schneebeli, M., Proksch, M., Schuttemeyer, D., Kern, M., and~~
701 ~~Davidson, M.W.J.: Nordic Snow Radar Experiment-, *Geosci. Instrum. Meth. Geoscientific-*~~
702 ~~*Instrumentation Methods and Data Systems*, 5, 403–415, <https://doi.org/doi:10.5194/gi-5-403-2016>,~~
703 ~~2016.~~

704 ~~L öwe H. and Picard, G.—“; Microwave scattering coefficient of snow in MEMLS and DMRT-ML~~
705 ~~revisited: The relevance of sticky hard spheres and tomography-based estimates of stickiness,”~~
706 ~~*Cryosphere*, vol. 9, no. (6), pp. 2101–2117, Nov. <https://doi.org/10.5194/tc-9-2101-2015>, 2015.~~

707 ~~Mabuchi, K., Sato, Y., Kida, H., Saigusa, N. and Oikawa, T.: A biosphere-atmosphere interaction~~
708 ~~model (BAIM) and its primary verification using grassland data, *Pap. Meteorol. Geophys.*, 47, 115–~~
709 ~~140, <https://doi.org/10.2467/mripapers.47.115>, 1997.~~

710 ~~Mortimer, C., Mudryk, L., Derksen, C., Luoju, K., Brown, R., Kelly, R., and Tedesco, M. : Evaluation~~
711 ~~of long-term Northern Hemisphere snow water equivalent products. *Cryosphere*, 14(5), 1579–1594,~~
712 ~~doi: 10.5194/tc-14-1579-2020, 2020.~~

713 ~~Naderpour, R., Schwank, M., Matzler, C., Lemmetyinen, J., and Steffen, K.: Snow Density and Ground~~
714 ~~Permittivity Retrieved From L-Band Radiometry: A Retrieval Sensitivity Analysis. *Ieee J-Stars. Ieee-*~~
715 ~~*Journal of Selected Topics in Applied Earth Observations and Remote Sensing*, 10(7), 3148–3161,~~
716 ~~<https://doi.org/doi:10.1109/Jstars.2017.2669336>, 2017.~~

717 ~~Pulliainen, J., Luoju, K., Derksen, C., Mudryk, L., Lemmetyinen, J., Salminen, M., Ikonen, J., Takala-~~
718 ~~M., Cohen, J., Smolander, T., and Norberg, J.: Patterns and trends of Northern Hemisphere snow mass-~~
719 ~~from 1980 to 2018. *Nature*, 581(7808), 294–298. doi: 10.1038/s41586-020-2258-0, 2020.~~

720 ~~Roesch, A.,~~
721 ~~Gilgen, H., Wild, M., and Ohmura, A.: Assessment of GCM simulated snow albedo using direct~~
722 ~~observations, *Clim. Dynam.*, 15, 405–418, <https://doi.org/10.1007/s003820050290>, 1999.~~

723 ~~Roy, A., Picard, G., Royer, A., Montpetit, B., Dupont, F., Langlois, A., Derksen, C., and Champollion,~~
724 ~~N.: Brightness Temperature Simulations of the Canadian ~~Seasonal-seasonal~~ *Snowpack-snowpack*~~
725 ~~*Driven-driven* by ~~Measurements-measurements~~ of the ~~Snow-snow~~ *Specific-specific* ~~Surface-surface~~~~
726 ~~*Areaarea-*, *Ieee T. Geosci. Remote. Ieee Transactions on Geoscience and Remote Sensing*, 51, 4692–~~
727 ~~4704, <https://doi.org/doi:10.1109/Tgrs.2012.2235842>, 2013.~~

728 ~~Royer, A., Roy, A., Montpetit, B., Saint-Jean-Rondeau, O., Picard, G., Brucker, L., and Langlois, A.:~~
729 ~~*Comparison of commonly-used microwave radiative transfer models for snow remote sensing, Remote*~~
730 ~~*Sens. Environ.*, 190, 247–259, <https://doi.org/10.1016/j.rse.2016.12.020>, 2017.~~

731 ~~Roy, A., Picard, G., Royer, A., Montpetit, B., Dupont, F., Langlois, A., Derksen, C., and Champollion,~~
732 ~~N.: Brightness Temperature Simulations of the Canadian ~~Seasonal~~ *Snowpack* ~~Driven by~~ *Measurements-*~~
733 ~~*of the Snow Specific Surface Area*, *IEEE T. Geosci. Remote*, 51, 4692–4704,~~
~~doi:10.1109/TGRS.2012.2235842, 2013~~

734 [Tedesco, M., and Kim, E.J.: Intercomparison of electromagnetic models for passive microwave remote](#)
735 [sensing of snow, *Ieee T. Geosci. Remote.*, 44, 2654-2666, <https://doi.org/10.1109/TGRS.2006.873182>,](#)
736 [2006.](#)

737 [Tedesco, M., Narvekar, P.S.: Assessment of the NASA AMSR-E SWE Product. *Ieee Journal of Selected*](#)
738 [Topics in Applied Earth Observations and Remote Sensing, 3, 141-159, doi:-](#)
739 [10.1109/Jstars.2010.2040462, 2010.](#)

740 [Vionnet, V., Brun, E., Morin, S., Boone, A., Faroux, S., Le Moigne, P., Martin, E., and Willemet, J.M.:](#)
741 [The detailed snowpack scheme Crocus and its implementation in SURFEX v7.2.-, *Geosci.entific Model*](#)
742 [Dev_elopment, 5, 773-791, <https://doi.org/doi-10.5194/gmd-5-773-2012>, 2012.](#)

743 [Xiao, L., Che, T., and Dai, L.Y.: Evaluation of Remote Sensing and Reanalysis Snow Depth Datasets-](#)
744 [over the Northern Hemisphere during 1980-2016. *Remote Sensing*, 12\(19\), doi: Artn-](#)
745 [325310.3390/Rs12193253, 2020.](#)

746 [Yang, Z.L., Dickinson, R.E., Robock, A., and Vinnikov, K.Y. : Validation of the snow submodel of the](#)
747 [biosphere-atmosphere transfer scheme with Russian snow cover and meteorological observational data,](#)
748 [Journal of Climate, 10, 353-373, \[https://doi.org/10.1175/1520-0442\\(1997\\)010<0353:Votsso>2.0.Co;2-\]\(https://doi.org/10.1175/1520-0442\(1997\)010<0353:Votsso>2.0.Co;2-\)](#)
749 [1997.](#)

750 [Zheng, D., Li, X., Zhao, T., Wen, J., van der Velde, R., Schwank, M., Wang, X., Wang, Z., and Su, Z.:-](#)
751 [Impact of Soil-soil Ppermittivity and Ttemperature Pprofile on L-Band Microwave-microwave](#)
752 [Emission-emission of Frozen-frozen Soilsoil. *Ieee T. Geosci. Remote.IEEE Transactions on-*](#)
753 [Geoscience and Remote Sensing, 59\(5\), 4080-4093, <https://doi.org/DOI->](#)
754 [10.1109/TGRS.2020.3024971, 2021.](#)

755 [Zhang, P., Zheng, D., van der Velde, R., Wen, J., Zeng, Y., Wang, X., Wang, Z., Chen, J., and Su, Z.:](#)
756 [Status of the Tibetan Plateau observatory \(Tibet-Obs\) and a 10-year \(2009-2019\) surface soil moisture](#)
757 [dataset-, *Earth Syst. Sci. Data*, 13, 3075-3102, <https://doi.org/10.5194/essd-13-3075-2021>, 2021.](#)

758 [Zheng, D., Li, X., Wang, X., Wang, Z., Wen, J., van der Velde, R., Schwank, M., and Su, Z.: Sampling](#)
759 [depth of L-band radiometer measurements of soil moisture and freeze-thaw dynamics on the Tibetan](#)
760 [Plateau-, *Remote Sens.ing of Environ.ment*, 226, 16-25,](#)
761 [https://doi.org/doi.org/10.1016/j.rse.2019.03.029, 2019.](#)